Molecular Ecology (2008) doi: 10.1111/j.1365-294X.2008.03879.x

Differential gene expression during thermal stress and bleaching in the Caribbean coral *Montastraea faveolata*

M. K. DESALVO,* C. R. VOOLSTRA,* S. SUNAGAWA,* J. A. SCHWARZ,† J. H. STILLMAN,‡ M. A. COFFROTH,§ A. M. SZMANT¶ and M. MEDINA*

**School of Natural Sciences, University of California, Merced, PO Box 2039, Merced, CA 95344, USA, †Department of Biology, Vassar College, 124 Raymond Avenue, Box 731, Poughkeepsie, NY 12604, USA, ‡Romberg Tiburon Center and Department of Biology, San Francisco State University, 3152 Paradise Drive, Tiburon, CA 94920, USA, §Graduate Program in Evolution, Ecology and Behaviour and Department of Geology, State University of New York at Buffalo, 447 Hochstetter Hall, Buffalo, NY 14260, USA, ¶Center for Marine Science, University of North Carolina Wilmington, 5600 Marvin K. Moss Lane, Wilmington, NC 28409, USA*

Abstract

The declining health of coral reefs worldwide is likely to intensify in response to continued anthropogenic disturbance from coastal development, pollution, and climate change. In response to these stresses, reef-building corals may exhibit bleaching, which marks the breakdown in symbiosis between coral and zooxanthellae. Mass coral bleaching due to elevated water temperature can devastate coral reefs on a large geographical scale. In order to understand the molecular and cellular basis of bleaching in corals, we have measured gene expression changes associated with thermal stress and bleaching using a complementary DNA microarray containing 1310 genes of the Caribbean coral *Montastraea faveolata*. In a first experiment, we identified differentially expressed genes by comparing experimentally bleached *M. faveolata* fragments to control non-heat-stressed fragments. In a second experiment, we identified differentially expressed genes during a time course experiment with four time points across 9 days. Results suggest that thermal stress and bleaching in *M. faveolata* affect the following processes: oxidative stress, Ca^{2+} homeostasis, cytoskeletal organization, cell death, calcification, metabolism, protein synthesis, heat shock protein activity, and transposon activity. These results represent the first medium-scale transcriptomic study focused on revealing the cellular foundation of thermal stress-induced coral bleaching. We postulate that oxidative stress in thermal-stressed corals causes a disruption of Ca^{2+} homeostasis, which in turn leads to cytoskeletal and cell adhesion changes, decreased calcification, and the initiation of cell death via apoptosis and necrosis.

Keywords: bleaching, coral, gene expression, microarray, thermal stress

Received 2 March 2008; revision received 26 June 2008; accepted 28 June 2008

Introduction

Coral reefs are important tropical marine ecosystems currently threatened by disease outbreaks (Harvell *et al*. 1999; Weil *et al*. 2006), overfishing and eutrophication (Hughes 1994; Jackson *et al*. 2001; Pandolfi *et al*. 2003), and mass bleaching events (Hoegh-Guldberg 1999). These factors will be exacerbated by future climate change (Hughes *et al*. 2003), and predictions of ocean acidification represent yet another threat to coral vitality (Hoegh-Guldberg *et al*. 2007). Coral bleaching describes the morphological changes that occur during the breakdown in symbiosis between the coral host and its dinoflagellate endosymbiont (*Symbiodinium* sp. or zooxanthellae). Upon bleaching, the coral host loses its coloration via the loss of its photosynthetic pigment-containing endosymbionts. The bleaching response can result from exposure to abnormal water temperature (e.g. Glynn 1993), pathogens (e.g. Kushmaro *et al*. 1996), high light and ultraviolet radiation (e.g. Gleason & Wellington 1993), a synergistic combination of multiple factors (e.g. Lesser & Farrell 2004), herbicides (Jones 2005), and other known stressors (reviewed in Douglas 2003). Of utmost importance is

Correspondence: Fax: 209-228-4060;
E-mail: mmedina@ucmerced.edu

thermal stress-induced coral bleaching, which is predicted to increase in intensity and frequency due to global warming (Hoegh-Guldberg 1999). Bleaching due to anomalously high seawater temperature can occur over a large geographical range (e.g. Berkelmans & Oliver 1999) and can lead to widespread coral mortality across the globe (Goreau *et al*. 2000).

A detailed description of the molecular and cellular events leading to bleaching is incomplete. It is possible that multiple mechanisms exist given that bleaching can result from a reduction in algal cell densities and/or a decrease in algal pigment concentration (e.g. Hoegh-Guldberg & Smith 1989; Fitt & Warner 1995). A decrease in algal density can occur via the detachment of host cells containing symbionts (Gates *et al*. 1992), necrosis and apoptosis of both host and symbiont cells (Dunn *et al*. 2002, 2004, 2007; Strychar *et al*. 2004; Richier *et al*. 2006), digestion of zooxanthellae by the coral host (Brown *et al*. 1995), and exocytosis of zooxanthellae (Steen & Muscatine 1987; Brown *et al*. 1995).

The events leading to a decrease in density of zooxanthellae is thought to begin with heat- and/or light-induced photoinactivation of photosystem II in the zooxanthellae (reviewed in Smith *et al*. 2005). Briefly, decreased photosynthesis in cultured zooxanthellae (e.g. Iglesias-Prieto *et al*. 1992) and zooxanthellae *in hospite* (e.g. Fitt *et al.* 1995; Warner *et al*. 1996) in response to elevated temperatures is thought to result from damage to the D1 protein of photosystem II (Warner *et al*. 1999; Lesser, Farrell 2004), or impairment of carbon dioxide fixation (Lesser 1996; Jones *et al*. 1998). The net result of either of these scenarios is the production of reactive oxygen species (ROS) by transport chain electrons (Hoegh-Guldberg 1999; Lesser 2006). Rampant ROS production is known to result in apoptosis/necrosis (e.g. Tiwari *et al*. 2002), and thus the production of ROS by photo-damaged zooxanthellae provides a mechanism by which environmental stressors can lead to degradation of the coral-algal symbiosis.

The use of molecular tools to assess the cellular basis of coral health has recently intensified. Investigated protein biomarkers consist mainly of heat shock proteins (HSP) and proteins involved in the oxidative stress response (see Table 2 in van Oppen & Gates 2006 for a comprehensive list of protein biomarkers). While HSPs may be potent biomarkers for assessing coral health in the field, their activities do not point to a mechanism of bleaching. However, both oxidative stress and nitric oxide signalling (Perez & Weis 2006) represent cellular pathways responsible for bleaching. Green fluorescent protein (GFP) homologues may also be involved in bleaching mechanisms. Although GFPs are thought to be photoprotective (Salih *et al*. 2000), and have also been shown to quench superoxide radicals (Bou-Abdallah *et al*. 2006), their expression appears to decrease during thermal stress (Dove *et al*. 2006; Smith-Keune & Dove 2008). In summarizing the available evidence, we can conclude that: (i) thermal stress results in HSP expression, GFP down-regulation, and oxidative stress; (ii) oxidative stress results in increased antioxidant protein expression and damage to DNA, lipids, and proteins; and (iii) oxidative stress and nitric oxide signalling are likely involved in the cellular basis of bleaching.

The emergence of complementary DNA (cDNA) microarrays for nonmodel organisms, which can assay the expression of thousands of genes simultaneously, has accelerated the discovery of stress-responsive genes and mechanisms in recent years (Gibson 2002; Gracey & Cossins 2003; Hofmann *et al*. 2005). Small-scale cDNA microarray approaches (32 genes) have been carried out with the scleractinian coral, *Montastraea faveolata*, exposed to environmental stress (Edge *et al*. 2005; Morgan *et al*. 2005). Large-scale microarray studies on marine organisms such as porcelain crabs (Teranishi & Stillman 2007), damselfish (Kassahn *et al*. 2007), mussels (Place *et al*. 2008), and gobies (Gracey *et al*. 2001; Buckley *et al*. 2006) have provided immense transcriptomic information in relation to thermal physiology. In this study, we report the first medium-scale cDNA microarray study on *M. faveolata* exposed to thermal stress and bleaching in a controlled laboratory setting. Differential gene expression was assessed during early stage thermal stress and partial bleaching. The results confirm HSP expression, GFP down-regulation and oxidative stress during bleaching; and also suggest that Ca^{2+} homeostasis, cytoskeletal dynamics, calcification, metabolism, and protein synthesis are affected by thermal stress and symbiosis breakdown.

Materials and methods

Field experiments

Two experiments were performed at the Smithsonian Tropical Research Institute's Bocas del Toro field station in Panamá during September and October 2006. The following apply to both experiments: (i) aquaria were exposed to shaded ambient light; (ii) aquaria were placed in large fiberglass ponds with continuous water flow to buffer temperature fluctuations; (iii) aquaria did not have running seawater but each contained a pump to generate continuous water flow; and (iv) heaters were used to raise the temperature in heated aquaria.

A single time point, single genotype thermal stress experiment ('experiment 1') was performed first. A large colony of *Montastraea faveolata* was collected near Isla Solarte (9°19′56.78″N and 82°12′54.65″W). A single colony was targeted in order to eliminate sources of variation from coral and zooxanthellae genotypes and thermal/light history (e.g. Brown *et al*. 2002; Rowan *et al*. 1997; Glynn *et al*. 2001). Ten coral 'plugs' were taken from the top of the

colony using a 2.5-cm diameter punch tool. The fragments were divided evenly between two identical 75-L aquaria, *c.* 25 cm deep, and kept at ambient temperature (29.23 ± 0.48 °C) for 3 days. After the acclimation period, two 200-W aquarium heaters were turned on in the experimental aquarium, which subsequently increased to 31.5 °C over 3 h. The average temperature of the experimental aquarium during the entire experiment was 32.23 ± 0.48 °C. HOBO Pendant Temperature/Light Data Loggers (Onset Corp UA-002-64) recorded temperature and light data every 3 min. These data loggers are not designed to measure photosynthetically active radiation (PAR, 400–700 nm), as only ~30% of the measured light is in the range of PAR. For this reason, relative light levels in the aquaria are reported (expressed as the percentage of the average 10 AM to 2 PM light intensity measured on a reef ~4 m deep in Bocas del Toro (9°22′68.4″N and 82°18′24.6″W) during September and October 2007). The control aquarium received slightly more light (37%) than the heated aquarium (28% of reef light). The experiment lasted 10 days and 17 h, after which all fragments were frozen in liquid nitrogen for molecular analysis. Immediately before freezing, a polyp-size tissue scraping (~12.6 mm^2) was preserved in 1 mL of 3.7% formaldehyde for zooxanthellae cell density analysis.

A time course experiment ('experiment 2') was conducted with four colonies of *M. faveolata* sampled from two separate reefs 21 km apart (two colonies from Isla Solarte – 9°19′56.78″N and 82°12′54.65″W, and two colonies from Cayos Zapatillas – 9°15′08.79″N and 82°02′24.63″W). Each colony was broken into eight fragments using a hammer and chisel. For each colony, four fragments were placed in a control aquarium, and four fragments were placed in an experimental aquarium fitted with two heaters, such that each colony was represented by a pair of aquaria (total of four control and four heated aquaria, all 75 L). After an acclimation period of 4 days at the natural temperature of the seawater system (mean temperature = 30.29 ± 0.07 °C), a fragment from each control and experimental aquaria was sampled as described above (time zero). After time zero sampling, the heaters in each of the experimental aquaria were turned on, and the rate of temperature increase was similar to experiment 1. The mean temperature of the control aquaria during the entire experiment was 29.74 ± 0.03 °C, and the mean temperature of the heated aquaria was 32.72 ± 0.32 °C. Control and experimental fragments were sampled again 1 day after turning on the heaters, at the first signs of slight bleaching (2 to 4 days after heating began, depending on coral genotype), and lastly, when all experimental fragments were partially bleached (9 days after heating began). All samples were taken at night. Light intensity differed slightly between the four aquaria fitted with HOBOs (control aquaria, 1–43%; control aquaria, 2–46%; heated aquaria, 1–35%; and heated aquaria, 2–34% of reef light).

Zooxanthellae cell counts and 18S restriction fragment length polymorphism analysis

The formaldehyde-fixed tissue scrapings were homogenized by maceration with a dissecting needle and vortexed. Cell counts were performed with a haemocytometer. For experiment 1, four replicate cell counts were performed per sample, averaged, and values adjusted to the number of cells per square centimetre. An independent samples *t*-test was performed to determine statistical significance between the two groups. For experiment 2, eight replicate cell counts were averaged for each coral genotype at each time point. After testing for normality and equal variances within time points, significance between time points was assessed using a one-way repeated measures ANOVA and Tukey post-hoc testing. All statistical tests were performed using SIGMASTAT 3.11.

Genomic DNA was isolated from frozen coral powder (see below) using the PowerPlant DNA Isolation kit (MoBio). The *Symbiodinium* 18S ribosomal subunit DNA was amplified using a universal forward primer (5′-GGTTGATCCTGCCAGTAGTCATATGCTTG-3′) and a zooxanthellae-specific reverse primer (5′-AGCACT-GCGTCAGTCCGAATAATTCACCGG-3′) following the protocols of Rowan & Powers (1991). The resulting 1.5-kb fragment was digested with *Taq*1 restriction enzyme, and the resulting fragments were compared to zooxanthellae clade standards (Rowan & Powers 1991).

RNA extraction and microarray hybridization

Total RNA from all frozen coral fragments was isolated using QIAzol lysis reagent (QIAGEN). Live tissue was chiseled off each coral fragment and homogenized using a prechilled mortar and pestle. Frozen coral powder was transferred directly to QIAzol. Two chloroform extractions were performed, followed by isopropanol precipitation and two washes in 80% ethanol. RNA pellets were redissolved in nuclease-free water and cleaned further with RNeasy Mini columns (QIAGEN). RNA quantity and integrity were assessed with a NanoDrop ND-1000 spectrophotometer and an Agilent 2100 Bioanalyser, respectively.

Microarray protocols followed those established by the Center for Advanced Technology at the University of California, San Francisco (http://cat.ucsf.edu/). One thousand three hundred and ten polymerase chain reaction (PCR)-amplified cDNAs from *M. faveolata* were spotted in duplicate on poly lysine-coated slides yielding a microarray with 2620 total features. Complementary DNAs were chosen from expressed sequence tags (EST) libraries described in Schwarz *et al*. (2008). To annotate the cDNAs, we performed a BLASTX analysis (*E*-value cut-off $1e^{-5}$) against the GenBank nonredundant DNA and protein database (nr). Before hybridization, microarrays were

postprocessed by (i) ultraviolet crosslinking at 60 mJ; (ii) a 'shampoo' treatment (3× SSC, 0.2% SDS at 65 °C); (iii) blocking with 5.5 g succinic anhydride dissolved in 335 mL 1-methyl-2-pyrrilidinone and 15 mL sodium borate; and (iv) drying via centrifugation.

For experiment 1, 1 μg of total RNA was amplified using the MessageAmp II aRNA kit (Ambion), and 3 μg of aRNA per sample were primed with 5 μg/μL random nonamer for 10 min at 70 °C. Reverse transcription (RT) lasted for 2 h at 42 °C using a master mix containing a 3:2 ratio of aminoallyl-dUTP to TTP. Following RT, single-stranded RNA was hydrolysed by incubating the RT reactions in 10 μL 0.5 M EDTA and 10 μL 1 M NaOH for 15 min at 65 °C. After hydrolysis, RT reactions were cleaned using Zymo Clean and Concentrator columns. Cy3 and Cy5 dyes (GE Healthcare) were dissolved in 17 μL dimethyl sulphoxide, and the coupling reactions lasted for 2 h at room temperature in the dark. Dye-coupled cDNAs were cleaned (Zymo), and appropriate Cy3- and Cy5-labelled cDNAs were mixed together in a hybridization buffer containing 0.25% SDS, 25 mM HEPES, and 3× SSC. The hybridization mixtures were boiled for 2 min at 99 °C then allowed to cool at room temperature for 5 min. The cooled hybridization mixtures were pipetted under an mSeries Lifterslip (Erie Scientific), and hybridization took place in Corning hybridization chambers overnight at 63 °C. Microarrays were washed twice in 0.6× SSC and 0.01% SDS followed by a rinse in 0.06× SSC and dried via centrifugation. Slides were immediately scanned using an Axon 4000B scanner. All aforementioned techniques were also conducted with coral fragments from experiment 2, omitting the initial RNA amplification, as total RNA quantity was adequate to prime 10 μg of total RNA with 5 μg/μL of Oligo-dT primer before RT.

Microarray data analysis

Experiment 1 followed a dye-swap design where each of the five control fragments was randomly paired to one of the five heat-stressed fragments. Each hybridization was performed twice with dye swapping between technical replicates, which allows for the control of dye labelling bias (Kerr 2003). Data analysis was performed using J/MAANOVA (Wu *et al*. 2003; Wu & Churchill 2005). Background-subtracted mean intensity values were $\log_2$ transformed and normalized using the spatial-intensity joint lowess algorithm. Following $\log_2$ transformation and lowess normalization, in-slide duplicate spots were collapsed by taking the mean. A fixed-effect MAANOVA model was fit to the intensity data with array, sample, and dye terms. Differentially expressed genes were identified by testing the sample term according to the empirical-Bayes F_S statistic (Cui *et al*. 2005). *P* values for each gene were generated by shuffling the residuals over 500 permutations. False discovery rate (FDR) adjustments were applied to the *P* values using a step-down FDR control method (Westfall & Young 1993), and genes were chosen at an adjusted alpha = 0.05.

Experiment 2 followed a reference design in which all heat-stressed RNA samples (four per time point) were compared to a pooled reference RNA sample composed of RNA from all control (untreated) coral fragments over all time points. Since all experimental RNA samples were compared to the reference sample, direct comparisons of gene expression across all time points can be performed. Background-subtracted mean intensity values were transformed and normalized as described above using J/MAANOVA. A MAANOVA fixed-effects model was fit to the intensity data with array and sample terms. Differentially expressed genes were identified using the same statistical methods described above. To visualize the temporal expression of differentially expressed genes, *K*-means clustering was performed using TIGR TMEV 4.0 software (Saeed *et al*. 2003). Microarray data from both experiments 1 and 2 have been deposited in Gene Expression Omnibus (GSE10680).

Quantitative real-time PCR

In order to validate microarray gene expression estimates, quantitative real-time PCR (qRT–PCR) was performed for seven genes chosen based on biological interest and to represent three classes of microarray data: (i) down-regulated > twofold; (ii) down-regulated < twofold; and (iii) up-regulated. SCRiP2, SCRiP8, and PXDN were > twofold down-regulated; EF-hand and C/EBPβ were < twofold down-regulated; MMP and AOSF722 were up-regulated. Complementary DNAs from experiment 1 (five nonbleached and five partially bleached) were synthesized from 1 μg of aRNA and diluted to a final volume of 200 μL. qRT–PCR primers (Table S1, Supplementary material) were designed using PRIMER EXPRESS 3.0 (Applied Biosystems), and test-PCRs confirmed specific amplification of the desired amplicons (70–100 bp). Two microlitres of cDNA were used in triplicate 12.5 μL qRT–PCRs with 0.2 μM primers and Power SYBR Green PCR Master Mix (Applied Biosystems) for 40 cycles. Delta cycle threshold (dCt) values were calculated by subtracting the Ct of a housekeeping gene (HKG) (CAON1295, a myosin) from the Ct's of the genes of interest. CAON1295 was the best-performing HKG from a group of candidates chosen from the microarray expression data. The quantitative methods used to identify candidate HKGs were identical to those reported by Rodriguez-Lanetty *et al*. (2007). Delta delta Ct (ddCt) values were calculated by subtracting the dCt's from nonbleached and bleached samples, and fold changes were calculated using the $2^{-\Delta\Delta Ct}$ method (Livak & Schmittgen 2001). Statistical significance between the two groups was assessed at the dCt level using a two-tailed *t*-test.

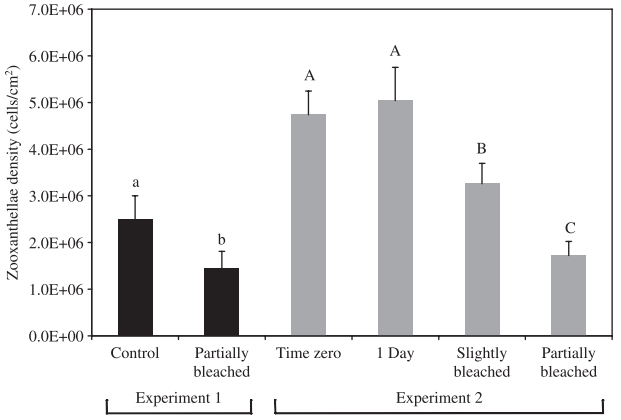

Fig. 1 Zooxanthellae cell count data from both experiments 1 and 2. The mean cell densities of five (experiment 1) or four (experiment 2) replicate fragments are shown with standard deviations. Letters above bars denote statistical significance — two means are significantly different ($P < 0.05$) if their letters are different. The difference between control and partially bleached in experiment 1 is statistically significant (independent samples *t*-test, $P < 0.001$). According to a one-way repeated measures ANOVA with Tukey post-hoc testing, all pair-wise comparisons in experiment 2 are significantly different with the exception of time zero vs. 1 day.

Results

Experiment 1: single colony, bleached vs. nonbleached

Thermal-stressed fragments at 32.2 °C were visibly paled after 3 days and continued to lose colour over the course of the experiment; however, they did not reach a fully bleached state. Algal cell density counts revealed that after nearly 11 days of thermal stress, experimental fragments contained an average of 1.44×10^6 ($\pm 5.02 \times 10^5$) cells/cm^2 compared to an average of 2.5×10^6 ($\pm 3.64 \times 10^5$) cells/cm^2 for controls (*t*-test, $P < 0.001$; Fig. 1). All control and heat-stressed fragments contained clade A zooxanthellae (data not shown).

Microarray analysis revealed large shifts in gene expression coincident with thermal stress and partial bleaching. MAANOVA identified 309 differentially expressed genes between untreated and thermal-stressed coral fragments (24% of all assayed genes). Of these 309 genes, 191 were up-regulated (higher expression during thermal stress), and 118 were down-regulated (lower expression during thermal stress) (Table S2, Supplementary material). Fold change magnitudes ranged from +1.9 to –4. Of the differentially expressed genes, only 21 up-regulated genes (11% of 191) and 47 down-regulated genes (39% of 118) had BLASTX hits ($E = 1 \times 10^{-5}$). Six members of a newly discovered scleractinian cysteine-rich, putatively secreted peptide family (SCRiPs) (S. Sunagawa, M. DeSalvo, C. Voolstra, A. Reyes-Bermudez & M. Medina, in preparation) were among the most highly down-regulated transcripts. Therefore, the function of 74 genes, or 24% of all genes identified as differentially expressed, were used to guide discussion on the transcriptomic response to thermal stress and bleaching (Table 1).

Differentially expressed genes presented in Table 1 are grouped according to gene ontology (GO) biological processes, cellular components, or manually defined categories. In addition, the putative functional roles are based on GO molecular functions, or manual definitions determined through literature searches and perusal of protein databases (e.g. PFAM and InterPro). Based on the molecular and cellular functions of the annotated genes, the following processes seem to be affected by thermal stress-induced bleaching: (i) extracellular matrix deposition; (ii) secretion of cysteine-rich peptides; (iii) oxidative stress; (iv) heat shock protein expression; (v) transposon activity; (vi) protein synthesis; (vii) organization of the actin cytoskeleton and cell adhesion; (viii) cell signalling; (ix) Ca^{2+} homeostasis; (x) nucleosome organization; and (xi) metabolism.

Experiment 2: multiple colonies, time course

Heat-treated corals at 32.72 ± 0.32 °C did not show any visible signs of bleaching after 1 day of elevated temperature. Slight bleaching of the four colonies did not occur simultaneously; one colony was slightly bleached after 2 days, two colonies after 3 days, and the fourth colony after 4 days. All thermal-stressed corals were partially bleached 9 days after beginning the experiment. Algal cell densities had declined by the slightly and partially bleached time points (Fig. 1). Cell densities of all later time points were statistically lower (ANOVA, $P < 0.001$) than time zero and 1 day, but there was no difference between time zero and 1 day cell densities. Algal cell densities in the control fragments also decreased during the experiment, albeit less than the heat-treated fragments. At slight bleaching (2 to 4 days), control fragments had 11% less zooxanthellae relative to the time zero baseline (heat-stressed fragments had 31% less zooxanthellae). At partial bleaching (9 days), control fragments had 29% less zooxanthellae relative to time zero (heat-stressed fragments had 64% less zooxanthellae). The loss of zooxanthellae in the control fragments was likely due to the low light levels present during the experiments. All control and heat-treated fragments for two of the colonies contained only clade A *Symbiodinium*. The two other colonies displayed high RFLP clade diversity ranging from only clade C to multiple clade mixes (data not shown).

Microarray analysis of experiment 2 was primarily focused on the temporal dynamics of genes that were differentially expressed upon heat treatment, that is, do the same genes identified in experiment 1 show temporal dynamics, or are they up-/down-regulated over all time

Table 1 Annotated differentially expressed genes from a replicate ($n = 5$) dye-swap experiment (experiment 1) comparing gene expression between partially bleached and control *Montastraea faveolata* fragments. Fold changes of gene expression are shown with F_s values, FDR-adjusted permutation P values, and qRT–PCR estimates (for six validated genes). Genes are grouped according to GO biological processes, GO cellular components, or manually defined categories. Functional roles are designated by GO molecular function or manually defined functions based on literature and database searches

GenBank Acc.	Clone ID	Annotation	Putative functional role	Fold Δ	F_s val	P val	qRT–PCR
Extracellular matrix proteins							
DR987943	AOSF1176	Galaxin	Soluble protein of the organic matrix	–3.45	71.52	0.000	
DR987689	AOSF997	Peroxidasin (PXDN)	ECM consolidation, peroxidase activity	–2.84	129.32	0.000	–10.36
DR988087	AOSF1268	Procollagen, type I, alpha 2	ECM structural constituent	–2.45	32.58	0.000	
DR987812	AOSF1095	SCP-like extracellular protein (SCP)	Ca2+ chelating serine protease	–1.88	42.83	0.000	
DR987160	AOSF561	Matrix metalloproteinase (MMP)	Metalloendopeptidase activity	1.53	28.43	0.000	2.74
Cysteine-rich peptide activity							
DR987097	AOSF513	Scleractinian cysteine-rich polypeptide 3A (SCRiP3A)	Unknown; secreted peptide	–3.99	68.52	0.000	
DR987884	AOSF1140	Scleractinian cysteine-rich polypeptide 5 (SCRiP5)	Unknown; secreted peptide	–3.62	54.24	0.000	
DR987486	AOSF810	Scleractinian cysteine-rich polypeptide 8 (SCRiP8)	Unknown; secreted peptide	–3.18	44.71	0.000	–22.14
DR987097	AOSF1192	Scleractinian cysteine-rich polypeptide 2 (SCRiP2)	Unknown; secreted peptide	–3.11	38.16	0.000	–6.53
DR987965	AOSF1190	Scleractinian cysteine-rich polypeptide 7 (SCRiP7)	Unknown; secreted peptide	–1.67	19.10	0.000	
DR987831	AOSF1109	Scleractinian cysteine-rich polypeptide 1 (SCRiP1)	Unknown; secreted peptide	–1.21	8.68	0.018	
Oxidative stress proteins							
DR988371	AOSF1447	Glutathione s-transferase mu (GST-M)	Detoxification of endogenous compounds	–1.29	10.46	0.009	
DR987313	AOSF666	Zinc RING finger protein 7 (SAG)	Lipid peroxide defense; protein ubiquitination	1.15	11.14	0.007	
DR987062	AOSF483	Glutathione S-transferase sigma-like (GST-S)	Detoxification of endogenous compounds	1.26	7.14	0.033	
Heat shock proteins							
DR988373	AOSF1451	90-kda heat shock protein (HSP90)	Refolding of denatured proteins	1.28	14.93	0.001	
DR987088	AOSF505	TCP-1 chaperonin family, zeta subunit (TCP-1)	Refolding of denatured proteins	1.36	30.02	0.000	
Ca^{2+} homeostasis proteins							
DR987851	AOSF1123	EF-hand domain protein	Ca2+ binding domain	–1.66	35.56	0.000	–2.58
DR987178	AOSF573	Calmodulin (CaM)	Ca2+ binding, adaptation of rhodopsin-mediated signalling	–1.38	16.56	0.001	
DR987514	AOSF836	FK506-binding protein 12 (FKBP12)	Refolding of denatured proteins; Ca2+ channel regulation	–1.35	33.49	0.000	
Cytoskeletal proteins/Cell adhesion molecules							
DR988150	AOSF1307	Gelsolin (GSN)	Calcium-regulated, actin-severing protein	–1.83	29.72	0.000	
DR986355	AOSB404	Tropomyosin (TPM)	Actin-binding cytoskeletal component	–1.52	9.45	0.014	
DR988440	CAOO655	Neurofascin homologue (NFASC)	Neural cell-cell adhesion	–1.32	10.27	0.010	
FE039783	CAON1906	Lethal giant larvae homologue 2 (LGL2)	Cytoskeleton organization, hemidesmosome assembly	–1.25	24.18	0.000	
DR988233	AOSF1357	Myosin 9A (MYO9A)	Actin-dependent ATPase activity	1.12	7.72	0.026	
DR987660	AOSF976	Fat tumor suppressor homologue 1 (FAT1)	Cadherin-mediated adhesion and signalling	1.14	9.30	0.014	
DR987650	AOSF969	Myosin 7A (MYO7A)	Actin-dependent ATPase activity	1.28	30.41	0.000	
Transposon activity							
DR988354	AOSF1434	PAZ domain/Piwi-like subfamily (PIWI)	Retrotransposon regulation	–1.51	12.70	0.004	
DR988240	CAON1787	Reverse transcriptase	Transcription of single-stranded RNA into cDNA	1.11	6.99	0.035	
DR988440	AOSF1490	Novel transposon	Transposable element activity	1.20	11.67	0.005	
FE039892	CAON537	Pol-like protein	Nuclease/transposase/RNase activity	1.23	8.45	0.020	
DR988412	AOSF1473	Reverse transcriptase	Transcription of single-stranded RNA into cDNA	1.30	13.34	0.003	
DR987618	AOSF 936	Reverse transcriptase	Transcription of single-stranded RNA into cDNA	1.33	9.27	0.014	
DR987618	AOSF1088	Reverse transcriptase	Transcription of single-stranded RNA into cDNA	1.52	38.90	0.000	

Table 1 *Continued*

GenBank Acc.	Clone ID	Annotation	Putative functional role	Fold Δ	F_s val	*P* val	qRT–PCR
Cell signalling proteins							
DR988240	AOSF1361	Rhodopsin-like G protein-coupled receptor	Rhodopsin-mediated signalling	−1.77	29.41	0.000	
DR987569	AOSF882	CCAAT/enhancer binding protein β (C/EBPβ)	Transcription factor activity	−1.52	25.38	0.000	−2.55
DR986829	AOSC957	Ets domain transcription factor (Pointed subfamily)	Transcription factor activity	−1.14	7.15	0.033	
Nucleosome/Transcription related proteins							
DR987246	AOSF622	H2A histone family, member V, isoform 1	Nucleosome assembly	−1.47	19.45	0.000	
DR988012	AOSF1219	Histone protein H3	Nucleosome assembly	−1.40	18.76	0.000	
DR988033	AOSF1233	Histone H2A, isoform 1	Nucleosome assembly	−1.28	6.24	0.047	
FE040071	CAON876	High mobility group AT-hook 2 (HMGA2)	Maintenance of chromatin architecture; transcriptional reg.	−1.21	8.50	0.019	
DR986454	AOSB760	SNF2 and DEXH-box helicase domain protein	Unwinding of DNA double helix	1.05	6.96	0.035	
FE039615	CAON1597	Bromodomain containing 8 (Brd8)	Component of histone acetylase complex	1.15	22.11	0.000	
Metabolic proteins							
FE040151	CAON999	Methionine adenosyltransferase 1α (MAT1α)	S-adenosylmethionine biosynthesis	−1.86	89.05	0.000	
DR988384	AOSF1456	Quinoid dihydropteridine reductase (QDPR)	Amino acid metabolism; tetrahydrobiopterin biosynthesis	−1.37	10.25	0.010	
FE040110	CAON943	NADH-ubiquinone oxidoreductase (NADH-ubiq)	Mitochondrial electron transport	−1.20	12.20	0.004	
DR987599	AOSF914	CDGSH iron sulfur domain 1	Iron transport into mitochondria	−1.18	11.67	0.005	
DR987302	AOSF657	Eukaryotic cobalamin-binding protein	Vitamin B12 binding and transport	−1.16	7.85	0.025	
FE039547	CAON1459	Ferritin (FTN)	Iron binding and homeostasis	−1.11	9.53	0.013	
Protein synthesis							
DR986615	AOSF1234	Ribosomal protein L9	Protein synthesis; structural constituent of ribosome	−1.47	7.42	0.029	
DR988446	AOSF1167	Ribosomal protein S3	Protein synthesis; structural constituent of ribosome	−1.34	11.91	0.005	
DR988446	AOSF1493	Ribosomal protein S5	Protein synthesis; structural constituent of ribosome	−1.31	24.70	0.000	
DR987242	AOSF620	Eukaryotic translation initiation factor	Regulation of translation initiation	−1.30	20.59	0.000	
DR988266	AOSF1376	Ribosomal protein S7	Protein synthesis; structural constituent of ribosome	−1.24	12.01	0.005	
DR987703	CAOO2477	Ribosomal protein L23	Protein synthesis; structural constituent of ribosome	−1.24	12.19	0.004	
DR988328	AOSF1416	Ribosomal protein X-linked	Protein synthesis; structural constituent of ribosome	−1.23	7.77	0.025	
DR986825	AOSC944	Ribosomal protein S25	Protein synthesis; structural constituent of ribosome	−1.23	7.62	0.027	
FE040377	CAOO2543	Splicing factor, arginine/serine-rich 4	Regulation of pre-mRNA splicing	−1.20	6.83	0.037	
DR987703	AOSF1009	Ribosomal protein L26	Protein synthesis; structural constituent of ribosome	−1.19	10.14	0.010	
DR986810	AOSC908	Ribosomal protein L12	Protein synthesis; structural constituent of ribosome	−1.18	21.94	0.000	
DR986717	AOSC713	Ribosomal protein L3	Protein synthesis; structural constituent of ribosome	−1.17	6.95	0.035	
DR988078	AOSF1264	Ribosomal protein L14	Protein synthesis; structural constituent of ribosome	−1.17	6.89	0.036	
DR986615	AOSC490	Ribosomal protein S2	Protein synthesis; structural constituent of ribosome	−1.14	8.64	0.018	
FE040562	CAOO902	Elongation factor 1α (EF1α)	Regulation of translation initiation	−1.12	16.13	0.001	
Miscellaneous proteins							
DR987865	AOSF1131	Green fluorescent protein homologue (GFP)	Energy transfer acceptor	−1.67	27.47	0.000	
DR988485	AOSF1521	USP-like protein	Universal stress protein (Bacteria)	−1.58	27.58	0.000	
DR987591	AOSF907	BPTI/Kunitz family of serine protease inhibitors	Serine-type endopeptidase inhibitor activity	−1.51	16.12	0.001	
DR986515	AOSB1028	Ubiquitin-conjugating enzyme E2S	Ubiquitination of proteins	−1.46	7.75	0.025	
FE040166	CAOO1050	Proline-rich protein	Unknown	−1.18	8.13	0.022	
DR988087	CAOO526	Probable transport protein sec61 alpha subunit	Protein targeting, transport, secretion	−1.14	6.26	0.046	
DR987207	AOSF595	Astacin domain containing protein	Zinc-regulated peptidase	1.09	31.45	0.000	
DR987088	AOSF387	Tachylectin-2 precursor	Lectin that binds N-acetyl-glucosamine and -galactosamine	1.10	7.14	0.033	
DR988170	AOSF1319	Zinc finger, NFX1-type containing 1	Zinc ion-binding transcription factor	1.12	7.86	0.024	
DR988384	CAON1194	Proline-rich salivary protein	Defense against plant polyphenolic compounds	1.22	7.57	0.028	
DR987159	AOSF560	Ubiquitin specific protease 24 (USP24)	De-ubiquitination of proteins	1.27	11.53	0.006	

points in a similar magnitude? Since all time zero and heat-stressed coral fragments were compared to the identical pooled reference RNA sample, we could directly compare levels of gene expression across time points. Using this approach, MAANOVA identified 280 differentially expressed genes, or 21% of all the genes on the microarray (Table S3, Supplementary material). Twenty-nine per cent of the 280 genes, or 81 total genes, were annotated by BLASTX.

Clustering of the differentially expressed genes grouped those behaving similarly over the time course. *K*-means clustering sorted the differentially expressed genes into eight clusters containing between 4 and 98 genes (Table S3). Figure 2 contains heat maps for the annotated genes within the eight clusters; however, since the majority of genes within clusters 5 and 6 are stably expressed across time points, only those annotated genes that show changes in gene expression are included in Fig. 2.

Genes within cluster 1 show large fold changes across the entire time course (mean expression profile = –1.4, –0.4, –0.2, –2.1); their expression at 1 day and slightly bleached is around twofold higher than time zero, and expression at partially bleached is around twofold less than time zero. These genes include the scleractinian cysteine-rich peptides (SCRiPs) and the extracellular matrix (ECM) component peroxidasin (PXDN); they represent the most down-regulated genes during bleaching. Genes within cluster 2 exhibit the same temporal pattern to cluster 1 but on a smaller scale (mean expression profile = –0.5, +0.1, +0.1, –0.7). Cluster 8 (mean expression profile = +0.2, –0.3, –0.2, +0.1) contains genes that show expression patterns opposite to those of clusters 1 and 2; expression at 1 day and slightly bleached is lower than time zero, and expression at partially bleached is slightly lower than time zero. Genes within cluster 3 show gene expression changes on the same scale as cluster 1, but in the opposite direction (mean expression profile = +0.3, +0.6, +1.7, +1.6). These genes are the most up-regulated during bleaching – their expression ramps up during early stage thermal stress but then levels off between slight and partial bleaching. Genes in cluster 7 are also among the most up-regulated during bleaching (mean expression profile = –0.5, +0.1, +0.2, +0.1). This cluster contains cell-signalling proteins [cylindromatosis protein (CYLD), a rhodopsin-like G protein-coupled receptor (GPCR), and protein-tyrosine phosphatase 4A1], and a heat-shock protein (TCP-1). Opposite to cluster 7 is cluster 4 (mean expression profile = +0.2, 0, 0, – 0.4) — these genes decrease in expression from time zero to 1 day and then decrease further from slight to partial bleaching. This cluster includes ribosomal proteins and two calcium-binding proteins [calmodulin (CaM) and an unknown EF-hand protein]. Finally, cluster 5 genes (mean expression profile = +0.1, +0.1, +0.2, +0.2) tend to increase during thermal stress, and cluster 6 genes tend to do the opposite (–0.1, –0.2, –0.2, and –0.1); although most genes in clusters 5 and 6 were remarkably stable across the time course.

Overlap between experiments 1 and 2

In response to thermal stress for 10 and 9 days, respectively, corals in experiments 1 and 2 became partially bleached. Given the similar endpoint in both experiments, a comparison was made of the differentially expressed genes. In total, 88 genes were differentially expressed in both experiments 1 and 2. Of these 88 genes, 57 genes show directionally consistent patterns of expression; 23 genes are consistently up-regulated, and 34 genes are consistently down-regulated (Table S4, Supplementary material). Annotated genes that were differentially expressed in experiments 1 and 2 showed both consistent patterns of gene expression (**, Fig. 2), and opposite patterns of gene expression (*, Fig. 2). In total, there are 19 annotated genes that yield similar results and five genes that yield opposite results between both experiments. Notable genes consistently down-regulated at partial bleaching are five SCRiPs, CaM, an unknown EF-hand protein, three ribosomal proteins, CCAAT/enhancer binding protein β (C/EBPβ), and a cobalamin-binding protein. Notable genes that are consistently up-regulated include glutathione S-transferase sigma (GST-S), TCP-1, tachylectin-2, and two reverse transcriptases.

Quantitative real-time PCR validation

The qRT–PCR-estimated fold changes of the seven tested genes were in the same direction as the microarray estimates, and dCt's of the nonbleached samples were statistically different from dCt's of the bleached samples (*t*-test, $P < 0.05$). For the six annotated genes, the qPCR estimates were inflated compared to the microarray results (Table 1). One non-annotated gene was tested (AOSF722), which had an array fold change = +1.7; its qRT–PCR result was deflated compared to the microarray (+1.4). At the ddCt level, we could assess the variation in qRT–PCR expression. Three genes greater than twofold down-regulated, SCRiP8 (mean ddCt 4.47 ± 1.3 SD), SCRiP2 (mean ddCt = 2.71 ± 0.65), and PXDN (mean ddCt = 3.37 ± 1.09), showed large variation in expression. Two genes less than twofold down-regulated, EF-hand (mean ddCt = 1.37 ± 0.64) and C/EBPβ (mean ddCt = 1.35 ± 0.91), and two genes up-regulated, MMP (mean ddCt = –1.46 ± 1.13) and AOSF722 (mean ddCt = –0.45 ± 0.45), also exhibited large variation in expression. Variation in qRT–PCR data was consistent with microarray estimates of variation (Table S5, Supplementary material). Overall, qRT–PCR results confirmed statistically significant differential expression of the seven genes tested and tended to yield expression estimates greater than those measured using the microarray.

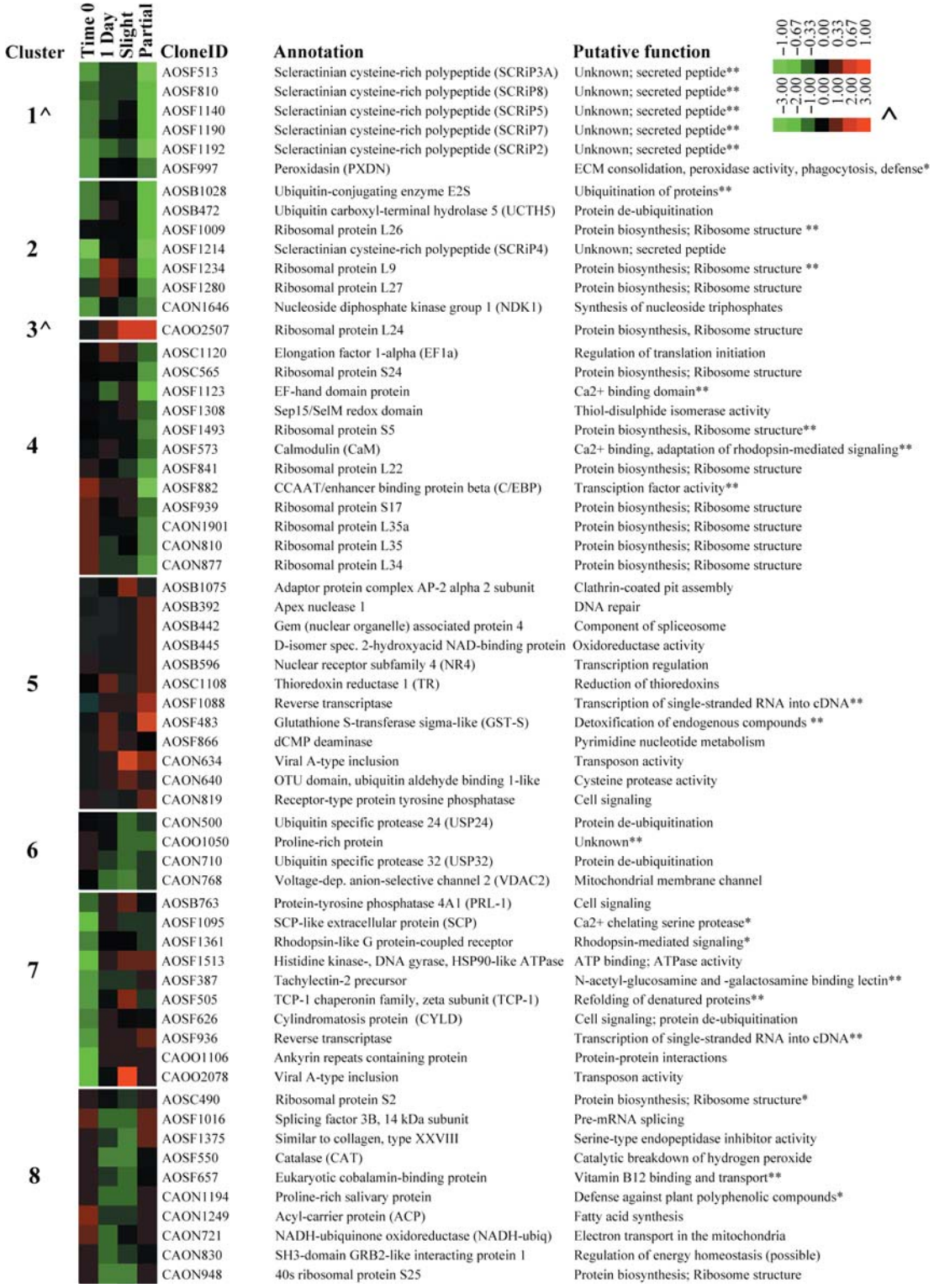

Cluster	CloneID	Annotation	Putative function
1^	AOSF513	Scleractinian cysteine-rich polypeptide (SCRiP3A)	Unknown; secreted peptide**
	AOSF810	Scleractinian cysteine-rich polypeptide (SCRiP8)	Unknown; secreted peptide**
	AOSF1140	Scleractinian cysteine-rich polypeptide (SCRiP5)	Unknown; secreted peptide**
	AOSF1190	Scleractinian cysteine-rich polypeptide (SCRiP7)	Unknown; secreted peptide**
	AOSF1192	Scleractinian cysteine-rich polypeptide (SCRiP2)	Unknown; secreted peptide**
	AOSF997	Peroxidasin (PXDN)	ECM consolidation, peroxidase activity, phagocytosis, defense*
2	AOSB1028	Ubiquitin-conjugating enzyme E2S	Ubiquitination of proteins**
	AOSB472	Ubiquitin carboxyl-terminal hydrolase 5 (UCTH5)	Protein de-ubiquitination
	AOSF1009	Ribosomal protein L26	Protein biosynthesis; Ribosome structure **
	AOSF1214	Scleractinian cysteine-rich polypeptide (SCRiP4)	Unknown; secreted peptide
	AOSF1234	Ribosomal protein L9	Protein biosynthesis; Ribosome structure **
	AOSF1280	Ribosomal protein L27	Protein biosynthesis; Ribosome structure
	CAON1646	Nucleoside diphosphate kinase group 1 (NDK1)	Synthesis of nucleoside triphosphates
3^	CAOO2507	Ribosomal protein L24	Protein biosynthesis, Ribosome structure
4	AOSC1120	Elongation factor 1-alpha (EF1a)	Regulation of translation initiation
	AOSC565	Ribosomal protein S24	Protein biosynthesis; Ribosome structure
	AOSF1123	EF-hand domain protein	Ca2+ binding domain**
	AOSF1308	Sep15/SelM redox domain	Thiol-disulphide isomerase activity
	AOSF1493	Ribosomal protein S5	Protein biosynthesis, Ribosome structure**
	AOSF573	Calmodulin (CaM)	Ca2+ binding, adaptation of rhodopsin-mediated signaling**
	AOSF841	Ribosomal protein L22	Protein biosynthesis; Ribosome structure
	AOSF882	CCAAT/enhancer binding protein beta (C/EBP)	Transciption factor activity**
	AOSF939	Ribosomal protein S17	Protein biosynthesis; Ribosome structure
	CAON1901	Ribosomal protein L35a	Protein biosynthesis; Ribosome structure
	CAON810	Ribosomal protein L35	Protein biosynthesis; Ribosome structure
	CAON877	Ribosomal protein L34	Protein biosynthesis; Ribosome structure
5	AOSB1075	Adaptor protein complex AP-2 alpha 2 subunit	Clathrin-coated pit assembly
	AOSB392	Apex nuclease 1	DNA repair
	AOSB442	Gem (nuclear organelle) associated protein 4	Component of spliceosome
	AOSB445	D-isomer spec. 2-hydroxyacid NAD-binding protein	Oxidoreductase activity
	AOSB596	Nuclear receptor subfamily 4 (NR4)	Transcription regulation
	AOSC1108	Thioredoxin reductase 1 (TR)	Reduction of thioredoxins
	AOSF1088	Reverse transcriptase	Transcription of single-stranded RNA into cDNA**
	AOSF483	Glutathione S-transferase sigma-like (GST-S)	Detoxification of endogenous compounds **
	AOSF866	dCMP deaminase	Pyrimidine nucleotide metabolism
	CAON634	Viral A-type inclusion	Transposon activity
	CAON640	OTU domain, ubiquitin aldehyde binding 1-like	Cysteine protease activity
	CAON819	Receptor-type protein tyrosine phosphatase	Cell signaling
6	CAON500	Ubiquitin specific protease 24 (USP24)	Protein de-ubiquitination
	CAOO1050	Proline-rich protein	Unknown**
	CAON710	Ubiquitin specific protease 32 (USP32)	Protein de-ubiquitination
	CAON768	Voltage-dep. anion-selective channel 2 (VDAC2)	Mitochondrial membrane channel
7	AOSB763	Protein-tyrosine phosphatase 4A1 (PRL-1)	Cell signaling
	AOSF1095	SCP-like extracellular protein (SCP)	Ca2+ chelating serine protease*
	AOSF1361	Rhodopsin-like G protein-coupled receptor	Rhodopsin-mediated signaling*
	AOSF1513	Histidine kinase-, DNA gyrase, HSP90-like ATPase	ATP binding; ATPase activity
	AOSF387	Tachylectin-2 precursor	N-acetyl-glucosamine and -galactosamine binding lectin**
	AOSF505	TCP-1 chaperonin family, zeta subunit (TCP-1)	Refolding of denatured proteins**
	AOSF626	Cylindromatosis protein (CYLD)	Cell signaling; protein de-ubiquitination
	AOSF936	Reverse transcriptase	Transcription of single-stranded RNA into cDNA**
	CAOO1106	Ankyrin repeats containing protein	Protein-protein interactions
	CAOO2078	Viral A-type inclusion	Transposon activity
8	AOSC490	Ribosomal protein S2	Protein biosynthesis; Ribosome structure*
	AOSF1016	Splicing factor 3B, 14 kDa subunit	Pre-mRNA splicing
	AOSF1375	Similar to collagen, type XXVIII	Serine-type endopeptidase inhibitor activity
	AOSF550	Catalase (CAT)	Catalytic breakdown of hydrogen peroxide
	AOSF657	Eukaryotic cobalamin-binding protein	Vitamin B12 binding and transport**
	CAON1194	Proline-rich salivary protein	Defense against plant polyphenolic compounds*
	CAON1249	Acyl-carrier protein (ACP)	Fatty acid synthesis
	CAON721	NADH-ubiquinone oxidoreductase (NADH-ubiq)	Electron transport in the mitochondria
	CAON830	SH3-domain GRB2-like interacting protein 1	Regulation of energy homeostasis (possible)
	CAON948	40s ribosomal protein S25	Protein biosynthesis; Ribosome structure

Fig. 2 Annotated differentially expressed genes from a replicate (n = 4) time course experiment (experiment 2) containing four time points. *K*-means clustering was performed to group genes by common temporal expression patterns. For clusters 1–4 and 7–8, only annotated genes are presented. For clusters 5 and 6, only those annotated genes that show changes in expression between time points are presented. Asterisks denote genes that were also differentially expressed in experiment 1 (Table 1): *opposite patterns of gene expression, and **similar patterns of gene expression between experiments 1 and 2. All clusters are on the scale of –1 to +1 $\log_2$ ratio (upper scale bar), except for clusters 1 and 3 (denoted by a ^), which are on the scale of –3 to +3 $\log_2$ ratio (lower scale bar).

Discussion

Using a cDNA microarray platform, we identified differentially expressed genes during thermal stress and bleaching. While thermal stress likely affects all cells, transcriptomic changes associated with the loss of symbionts may be confined to the gastrodermal cells — the primary zooxanthellae-harboring cells. Low fold changes in some genes may reflect dilution of mRNA abundances for processes occurring only in symbiotic cells (Rodriguez-Lanetty *et al*. 2006), while larger fold changes may reflect processes occurring in both symbiotic and nonsymbiotic cells (e.g. cells of the epithelium and calicoblastic epithelium). It is likely, also, that both control and thermally stressed coral fragments experienced stress involved in transplantation from the reef and changes associated with aquarium conditions (e.g. low light levels). As a result, it is likely that a stress response was present in both control and experimental corals, perhaps masking the degree of gene expression changes due to thermal stress alone. However, there were clear expression patterns associated with the thermal stress conditions that speak to the biology of corals that are subjected to conditions that cause bleaching.

qRT–PCR validation of six genes yielded fold change values on average three times greater than the microarray fold change estimates. Compression of microarray-estimated fold changes relative to qRT–PCR estimates are reported repeatedly in both technique-driven (e.g. Rajeevan *et al*. 2001; Yuen *et al*. 2002; Dallas *et al*. 2005; Wang *et al*. 2006) and functional genomics literature (e.g. Covarrubias *et al.* 2005; Hawkins *et al*. 2007). Reasons for microarray-based fold change compression include the level of gene expression (i.e. reduced agreement occurs in genes with very high or very low levels of gene expression), and location of qRT–PCR primers (i.e. reduced agreement when there is large separation between the location of the primers and microarray probes) (Etienne *et al*. 2004). Furthermore, the normalization method can have an effect on the agreement between microarray and qRT–PCR data. For example, Wang *et al*. (2006) found that fold change compression was more evident when lowess normalization was used (i.e. the normalization method utilized in the present study).

A striking observation from experiment 1 is that even though more genes were up-regulated (191) than down-regulated (118), only 10% of the up-regulated genes are annotated, whereas 40% of the down-regulated genes are annotated by BLASTX. While this may be due to chance, it could be suggestive of coral-specific genes and processes being up-regulated during bleaching, and evolutionarily conserved cellular processes being down-regulated during bleaching. Many non-annotated (NA) genes displayed large fold changes (Tables S2 and S3). NA genes may represent ESTs that contain mainly untranslated regions, or they may be coral-specific genes. The sequencing of the *Nematostella vectensis* genome (Putnam *et al*. 2007) has been beneficial to coral genomics; however, given the future growth of coral functional genomic analyses, our ability to formulate meaningful conclusions will be greatly enhanced by a coral genome project.

While 57 genes show consistent patterns of gene expression at a partially bleached state, it is notable that there is no higher overlap between the results of experiments 1 and 2. Given the differing designs of the two experiments (i.e. single colony, single time point vs. multicolony, time course), we did not expect to see high overlap. Additionally, the four colonies in experiment 2 were not uniform in their symbiont genotype. Although never shown before, the clade of *Symbiodinium* within the coral host may strongly influence host gene expression. This factor is likely another reason why we see different stress-induced gene expression in both experiments. Nevertheless, the activities of the genes listed in Table S4 and the annotated genes with a double asterisk in Fig. 2 reveal stunning, consistent heat stress-induced gene expression patterns. Genes such as CaM, the SCRiPs, EF-hand, C/EBPβ and PXDN are prime candidates for future work on protein function and localization.

A transcriptome-based bleaching model

Heat shock proteins (HSP)

Figure 3 illustrates a putative model of bleaching based on past studies and the present findings. The induction of HSPs is a hallmark of the heat shock response (reviewed in Lindquist 1986). As expected, transcriptomic data suggest increased HSP activity in heat-stressed *Montastraea faveolata*. Both HSP90 and a TCP-1 chaperonin homologue show increased expression in experiment 1 (Table 1). The same TCP-1 gene is differentially expressed in experiment 2 — as a member of cluster 7 (Fig. 2), its expression at all later time points is greater than its expression at time zero. The expression level of TCP-1 at slight bleaching is nearly twofold greater than at time zero. These results are in accordance with previous studies reporting the induction of heat shock proteins during heat stress (Black *et al*. 1995; Hayes & King 1995; Fang *et al*. 1997; Sharp *et al*. 1997; Gates & Edmunds 1999; Downs *et al*. 2000, 2002, 2005).

Oxidative stress and nitric oxide signalling

Thermal stress, in synergy with normal to high light levels, leads to the production of ROS in the plastids of zooxanthellae (reviewed in Hoegh-Guldberg 1999; Lesser 2006). The low light levels present during our experiments suggest that the observed bleaching response may not be reflective of natural bleaching events. In the absence of research-grade PAR measurements, Fv/Fm data, and/or

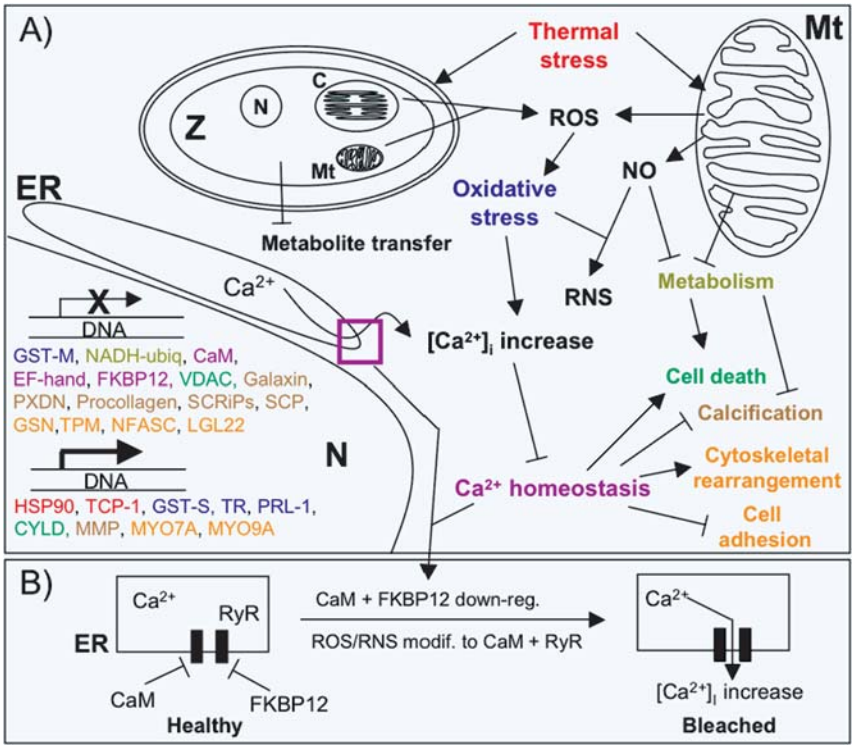

Fig. 3 (A) A proposed model of cellular processes leading to coral bleaching. Thermal stress leads to reactive oxygen species (ROS) formation in the electron transport chains of the zooxanthellae (Z) plastids (C), and the mitochondria (Mt) of both coral and zooxanthellae. ROS cause oxidative stress in the coral cell, the formation of reactive nitrogen species (RNS) in combination with nitric oxide (NO), and a disruption of Ca^{2+} homeostasis (marked by a rise in intracellular Ca^{2+}). Disruption of Ca^{2+} homeostasis causes cytoskeletal rearrangement, cell adhesion changes, decreased calcification, and the initiation of cell death. Thermal and oxidative stress in both coral and zooxanthellae lead to decreased metabolism, which also contributes to decreased calcification and cell death. Colour-coding is meant to connect cellular processes with differentially expressed genes reported in this study. ER, endoplasmic reticulum, and N, nucleus. For gene abbreviations, see Table 1 and Fig. 2. (B) A mechanism by which oxidative stress can lead to a disruption in Ca^{2+} homeostasis. In healthy cells, calmodulin (CaM) and FKBP12 inhibit the activity of ryanodine receptors (RyRs) such that Ca^{2+} is only released from the ER during necessary Ca^{2+} signalling events. Our data show that both CaM and FKBP12 are down-regulated during bleaching. These findings, in addition to published reports showing that oxidative stress leads to oxidative modifications to CaM and RyRs, suggest that RyR regulation is inhibited in bleached corals.

direct measurements of ROS, we cannot determine whether the corals in these experiments experienced oxidative stress conditions thought to induce bleaching when high light is present. It is known, however, that the mitochondrial respiratory chain is a site of ROS generation (Cadenas & Davies 2000; Davidson & Schiestl 2001). Thermal stress-induced mitochondrial ROS generation has been shown in nonphotosynthetic organisms, such as yeast (Davidson *et al*. 1996), clams (Abele *et al*. 2002), and human keratinocytes (Shin *et al*. 2008). Even though light levels present during these experiments may not have been high enough to induce significant ROS generation in zooxanthellae plastids, oxidative stress in the coral host is supported given the influence of thermal stress on the mitochondria of both the coral and zooxanthellae.

Regardless of their source, ROS are highly reactive and lead to lipid, protein, and DNA damage. Numerous studies have shown an increased antioxidant response in corals during stress. For example, superoxide dismutase was increased during thermal stress (e.g. Downs *et al*. 2000, 2002; Lesser & Farrell 2004). Downs *et al*. (2000) established that lipid peroxidation (oxidative damage of lipids) increased during thermal stress, and that glutathione levels decreased during thermal stress. A slight increase in catalase (CAT) during heat and light stress has also been shown in the zoanthid, *Palythoa caribaeorum* (Lesser *et al*. 1990). We found up-regulated expression of oxidative stress genes in the present experiments — glutathione s-transferase sigma (GST-S) in experiments 1 and 2, and thioredoxin reductase 1 (TR-1) and CAT in experiment 2. The up-regulation of glutathione s-transferase sigma (GST-S) is suggestive of increased detoxification of ROS. GST-S catalyses the conjugation of lipid peroxides to glutathione in *Drosophila* (Singh *et al*. 2001). In addition, the up-regulation of TR-1 is a sign of oxidative stress; TR-1 is responsible for keeping thioredoxin in a reduced state capable of detoxifying

oxidized molecules (Holmgren 1985). The down-regulation of glutathione s-transferase mu (GST-M) in experiment 1 is counter-intuitive since this class of GST is well known to be inducible by oxidative stress and active in the detoxification of ROS (Hayes & McLellan 1999). It is possible that GST-M was down-regulated due to the exhaustion of the cellular glutathione pool, or that GST-M in *M. faveolata* functions in roles not related to oxidative stress (Hayes *et al.* 1999). Besides the 'classical' oxidative stress genes mentioned already, protein tyrosine phosphatase 4A1 [also known as phosphatase of regenerating liver-1 (PRL-1)], a member of cluster 7, is consistently up-regulated at all time points relative to time zero. A recent study showed that mRNA and protein expression of PRL-1 was increased during oxidative stress in cultured mammalian retinal cells (Yu *et al*. 2007).

Nitric oxide (NO) production by the cnidarian host in response to thermal and oxidative stress may be involved in the breakdown in symbiosis; exposure to high temperature led to an increase in NO production by symbiotic anemones followed by bleaching (Perez & Weis 2006). Additionally, zooxanthellae nitric oxide synthase activity was shown to be associated with coral bleaching (Trapido-Rosenthal *et al*. 2005). While NO can be involved in normal cell signalling processes, in the presence of ROS, reactive nitrogen species (RNS) can be formed (e.g. peroxynitrite), which have the same damaging qualities as ROS. Furthermore, NO specifically inhibits mitochondrial NADH-ubiquinone reductase activity (Riobo *et al*. 2001), which directly inhibits ATP production. The collected detriments of ROS, RNS, and NO must invariably lead to diminished metabolism of the coral host. Our results suggest thermal stress and bleaching negatively affect coral host metabolism. Down-regulation of NADH-ubiquinone oxidoreductase (NADH-ubiq) subunits in both experiments (Table 1 and cluster 8) suggests deficiencies in mitochondrial electron transport. Additionally, down-regulation of acyl-carrier protein (cluster 8) points to a decrease in fatty acid synthesis, and down-regulation of both methionine adenosyltransferase 1α and quinoid dihydropteridine reductase (Table 1) suggest decreased amino acid metabolism. While decreased metabolism may be connected to the action of ROS, RNS, and NO, we cannot downplay the role of nutrient exchange between host and symbiont. Zooxanthellae translocate 95% of their photosynthates to the coral (Muscatine 1990), and they supply their host with a wide range of necessary compounds (Trench 1979). The lack of nutrient exchange between the coral and zooxanthellae during bleaching could also result in decreased metabolism of the coral.

Disruption of intracellular Ca^{2+} homeostasis

Intracellular Ca^{2+} homeostasis is critical to a functioning cell as Ca^{2+} is a ubiquitous cell messenger. Oxidative stress can disrupt Ca^{2+} homeostasis (Loven 1988; Orrenius *et al*. 1992). This disruption is marked by a sustained elevation in intracellular Ca^{2+} due to both the release of Ca^{2+} from intracellular stores and the entry of extracellular Ca^{2+}. Evidence from our experiments points to a disruption of Ca^{2+} homeostasis during bleaching, which is exemplified by the down-regulation of calmodulin (CaM) and an EF-hand protein. CaM is a ubiquitous protein that transduces Ca^{2+} signals via four EF-hands (Ca^{2+}-binding domains); conformational change upon Ca^{2+} binding allows CaM to bind effector molecules. Given the importance of Ca^{2+} signalling in numerous cellular processes, it is surprising that CaM is consistently down-regulated in bleached *M. faveolata*. However, oxidative stress in human skin cells disabled CaM from binding Ca^{2+} and led to decreased CaM expression (Schallreuter *et al*. 2007). Given that CaM interacts with members of all families of Ca^{2+} channels at the plasma membrane, ER and mitochondria (reviewed in Kasri *et al*. 2004), disruption of CaM function during oxidative stress would have profound effects on Ca^{2+} homeostasis.

The down-regulation of FKBP12 further supports the notion of disrupted Ca^{2+} homeostasis in bleached *M. faveolata*. FKBP12 modulates the Ca^{2+} flux properties of ryanodine receptors (RyR); RyRs are Ca^{2+} release channels found on all intracellular Ca^{2+} storing organelles (reviewed in Fill & Copello 2002). Binding of both FKBP12 and CaM to a RyR inhibits channel activity, while their removal activates the channel. Moreover, ROS and RNS modify RyRs and thus alter their activity (Hidalgo 2005). These findings suggest that the Ca^{2+} releasing activities of RyRs are altered during oxidative stress via (i) the down-regulation of FKBP12 and CaM, (ii) the inability of CaM to bind Ca^{2+}, and (iii) oxidative modifications to RyRs (Fig. 3B). NO can also cause an increase in Ca^{2+} by activating the release of Ca^{2+} from mitochondria (Richter 1998), thus providing another mechanism by which Ca^{2+} homeostasis can become disrupted during bleaching.

The role of Ca^{2+} in coral bleaching has been explored previously. Sustained increases in intracellular Ca^{2+} during thermal stress were measured over 6 h (Fang *et al*. 1997) and 24 h (Huang *et al*. 1998) in isolated coral cells. Both studies found that intracellular Ca^{2+} stores were released during heat treatment, and that bleaching required a continuous exogenous supply of Ca^{2+}. Sawyer & Muscatine (2001) used Ca^{2+} channel blockers, Ca^{2+} ionophores, and CaM antagonists to study cold-shock induced bleaching via cell detachment in *Aiptasia*. Interestingly, caffeine treatment (which releases Ca^{2+} from intracellular stores) caused bleaching over 1.5–2.5 h, but an increase in intracellular Ca^{2+} was not measured during the first 12 min of caffeine treatment in isolated cells. Ca^{2+} imaging studies over the timescale of days/weeks of thermal stress are needed in order to unequivocally support the hypothesis of Ca^{2+} homeostasis disruption during coral bleaching.

Modifications to the actin cytoskeleton and cell adhesion

The proposed model of bleaching (Fig. 3) follows a scheme where thermal stress, oxidative stress, NO signalling, disruption of Ca^{2+} homeostasis, and decreased metabolism lead to cytoskeletal rearrangement, changes in cell adhesion properties, decreased calcification, and cell death. Cytoskeletal elements are themselves sensitive to damage by thermal stress (e.g. Muller *et al*. 2007), and a hallmark of Ca^{2+} homeostasis breakdown due to oxidative cell injury is a disruption of the actin cytoskeleton (Loven 1988; Orrenius *et al*. 1992). Five genes associated with the actin cytoskeleton are differentially expressed in *M. faveolata* during thermal stress and bleaching. Gelsolin (GSN), lethal giant larvae 2 (LGL2), and tropomyosin (TPM) are down-regulated in response to thermal stress; whereas, myosin 7 A (MYO7A) and myosin 9 A (MYO9A) are slightly up-regulated. GSN, an actin filament capping and severing protein, and TPM, also an actin-binding protein, are both regulated by intracellular Ca^{2+} (Janmey & Stossel 1987; Lees-Miller & Helfman 1991). LGL2 is a heavily studied gene with homologues present in *Drosophila*, yeast, zebrafish, and mammals where it is involved in cytoskeletal organization (Strand *et al*. 1994). Myosins are a large family of actin-binding motor proteins that mediate various cellular processes. The expression of the aforementioned five genes most likely represents re-organization (or disruption due to thermal damage) of the actin cytoskeleton as a result of thermal stress, oxidative stress, and the disruption of Ca^{2+} homeostasis. It is likely that the cytoskeleton is also reorganized upon thermal stress due to the modulation of cell volume coincident with osmotic stress responses (reviewed in Mayfield & Gates 2007).

Various studies have also implicated LGL2 in cell adhesion processes. For example, the zebrafish homologue is involved in hemidesmosome formation (Sonawane *et al*. 2005) — hemidesmosomes are essential to the adhesion between cells and their underlying extracellular matrix (reviewed in Litjens *et al*. 2006). LGL2 mutants in *Drosophila* confirmed its role in cell adhesion. Both Gateff (1978) and Agrawal *et al*. (1995) showed that cell–cell contacts were defective in the absence of functional LGL2. In their description of LGL2, Strand *et al*. (1994) reasoned that all of the defective cell adhesion symptoms associated with LGL2 mutation could be attributed to the disruption of the cytoskeleton network.

The dual activities of LGL2 in cytoskeletal organization and cell adhesion are reflective of cell adhesion molecules that contain cytoplasmic actin-binding domains or interact with cytoplasmic actin-binding proteins (Halbleib & Nelson 2006; Delon & Brown 2007). We postulate that the differential expression of LGL2 in bleached *M. faveolata* illustrates how disrupted Ca^{2+} homeostasis due to oxidative stress can have effects on both the cytoskeleton and cell adhesion. In addition, a neurofascin (NFASC) homologue is down-regulated in bleached *M. faveolata*. This gene is likely a member of the L1 family of immunoglobulin (Ig) cell adhesion molecules, which are usually implicated in neural cell adhesion (Brummendorf *et al*. 1998). The topic of cell adhesion in the context of coral bleaching is relevant given that one proposed mechanism of bleaching involves detachment of gastrodermal cells containing zooxanthellae (Gates *et al*. 1992).

Cell death

Unabated oxidative stress can lead to cell death (e.g. Tiwari *et al*. 2002), and thus the mounting evidence of oxidative mechanisms involved in bleaching is consistent with recent findings of apoptosis and necrosis in heat-stressed zooxanthellae and cnidarian hosts (Dunn *et al*. 2002, 2004, 2007; Strychar *et al*. 2004; Richier *et al*. 2006). An uncontrolled increase in intracellular Ca^{2+} can lead to apoptosis (Duchen 2000; Hajnoczky *et al*. 2003; Orrenius *et al*. 2003). For example, when elevation of mitochondrial Ca^{2+} occurs in cells during oxidative stress (since Ca^{2+} channels are modified by ROS/RNS), mitochondrial rupture occurs leading to the release of mitochondrial contents into the cytoplasm and the initiation of cell death. The decision between apoptotic or necrotic modes of cell death is thought to depend on the nature of the stress and the amount of ATP present in the cell (Orrenius *et al*. 2003). Necrosis proceeds when both intracellular energy levels and mitochondrial function are severely degraded, while apoptosis proceeds during the opposite conditions (Nicotera *et al*. 1998). Both cell death responses have been documented during thermal bleaching in *Aiptasia* (Dunn *et al*. 2002, 2004), and necrotic tissue has been observed repeatedly in histological sections of bleached corals (e.g. Lasker *et al*. 1984; Glynn *et al*. 1985; Szmant & Gassman 1990; Brown *et al*. 1995). While our data cannot differentiate between the two modes of cell death, it is important to emphasize that oxidative stress and a disruption in Ca^{2+} homeostasis can lead to both outcomes.

It would have been quite informative to see expression patterns for critical genes in the apoptotic pathway, such as the cell cycle protein p53, an upstream regulator of apoptosis (Lesser & Farrell 2004), and Bcl-2 and caspase homologues (Dunn *et al*. 2006). Unfortunately, these genes are not present on the microarrays that were used in this study. Their absence is likely a result of the conditions under which the cDNA libraries were made.

Although the microarrays used in this study do not contain classical pro-apoptotic genes (e.g. APAF-1, Bax, and Bad in addition to those mentioned previously), differentially expressed genes identified in the present experiments are suggestive of apoptosis. The down-regulation of voltage-dependent anion-selective channel 2 (VDAC2) in experiment 2 is pro-apoptotic (see cluster 6). This anion

channel inhibits Bak activation and mitochondrial apoptosis (Cheng *et al*. 2003; Chandra *et al*. 2005); thus, down-regulation of VDAC2 suggests the activation of mitochondrial apoptosis. Additionally, the cylindromatosis (CYLD) gene is a member of cluster 7, and thus consistently up-regulated at all time points relative to time zero. CYLD is a de-ubiquitinating enzyme not involved in the ubiquitin-proteasome system. The de-ubiquitinating activities of CYLD are numerous (Simonson *et al*. 2007); however, CYLD up-regulation leads to apoptosis. Brummelkamp *et al*. (2003) reported that knockdown of CYLD led to activation of NFkB, which is antiapoptotic. The negative regulation of NFkB by CYLD has been further dissected: de-ubiquitination of TRAF2 (Kovalenko *et al*. 2003) and NEMO (Kovalenko *et al*. 2003; Nijman *et al*. 2005) by CYLD led to the de-activation of NFkB. Most recently, Xue *et al*. (2007) showed that de-ubiquitination of dTRAF2 (the *Drosophila* homologue of TRAF2) by CYLD leads to JNK-dependent apoptosis. These results suggest that up-regulation of CYLD over the time course of thermal stress is a pro-apoptotic signal.

Decreased calcification

The sharp down-regulation of proteins localized to the ECM suggests that the ECM of thermal-stressed corals is structurally different from that of healthy corals. These proteins are thought to be involved in the synthesis of the organic matrix, which is necessary for calcification (Allemand *et al*. 1998). Decreased calcification resulting from thermal stress was first observed over 25 years ago in both natural (Hudson 1981) and laboratory settings (Jokiel & Coles 1977; Coles & Jokiel 1978). Bleached corals presumably undergo lower rates of skeletogenesis than healthy corals due to the involvement of zooxanthellae in calcification, a phenomenon known as light-enhanced calcification (reviewed in Allemand *et al*. 2004). The absence of zooxanthellae does indeed affect the composition of the organic matrix (Cuif *et al*. 1999). A recently described protein found in the organic matrix of *Galaxea fascicularis*, named galaxin (Fukuda *et al*. 2003), is highly down-regulated in bleached *M. faveolata* (Table 1). The down-regulation of galaxin, along with that of peroxidasin, procollagen, and an SCP-like extracellular protein, suggests that the ECM of bleached *M. faveolata* is changing in composition to reflect their bleached state. Furthermore, the up-regulation of a matrix metalloproteinase (MMP) suggests increased degradation of the ECM (Shapiro 1998). Although the functions of the scleractinian cysteine-rich peptides (SCRiPs) are unknown, their secreted nature, down-regulation during bleaching, and clustering with known ECM components (data not shown), point to a potential role of these peptides in the process of calcification (S. Sunagawa, M. DeSalvo, C. Voolstra, A. Reyes-Bermudez & M. Medina, in preparation). Calcification is an energy-intensive process as the coral must actively pump Ca^{2+} to the calicoblastic epithelium (Tambutte *et al*. 1996). While decreased metabolism can explain a decrease in calcification during bleaching, a disruption in Ca^{2+} homeostasis must also be involved since the activity of all cellular Ca^{2+} pumps can be compromised by ROS, RNS, and CaM dysfunction.

Novel responses during thermal stress and bleaching

One of the most striking results from both experiments is the down-regulation during bleaching of transcripts involved in mRNA translation (mainly ribosomal proteins). In experiment 1, 12 ribosomal proteins, elongation factor 1α (EF1α), eukaryotic translation initiation factor, and an mRNA splicing factor are down-regulated. In experiment 2, cluster 2 contains three ribosomal proteins that increase at 1-day and slight bleaching and decrease at partial bleaching relative to time zero. Cluster 4 contains seven ribosomal proteins and EF1α that decrease at all time points relative to time zero. Contrary to these results is ribosomal protein L24 (see cluster 3), which is highly up-regulated at all time points relative to time zero. This contradictory result is probably indicative of continued protein synthesis during thermal stress and bleaching. However, as a whole, these results suggest that after 9–10 days of thermal stress and significant bleaching, a marked down-regulation of many components of protein synthesis occurred. Similar findings are reported with model organisms: heat shock led to a temporary down-regulation of ribosomal protein transcription in yeast (Herruer *et al*. 1988), and an inhibition of ribosomal protein translation in *Drosophila* (Bell *et al*. 1988).

Another unexpected result is the apparent increase in transposable element (TE) activity during bleaching. The up-regulation of a transposon, a pol-like protein, and four reverse transcriptase genes in bleached *M. faveolata* during experiment 1 supports this notion. In experiment 2, two viral A-type inclusion genes are up-regulated at all thermal stress time points relative to time zero (CAON634 in cluster 5 and CAOO2078 in cluster 7), and two reverse transcriptase genes are up-regulated at all time points relative to time zero (AOSF1088 in cluster 5 and AOSF936 in cluster 7). These findings relate to seminal work showing that maize TEs became active during chromosomal breakage (McClintock 1950). Further research on plants has shown that TEs are activated upon numerous stressors (McClintock 1984), and virtually all known plant retrotransposons are activated by stress (Wessler 1996). Moreover, thermal stress activated TEs in *Drosophila* (Ratner *et al*. 1992), silkworm (Kimura *et al*. 2001), black tiger shrimp (de la Vega *et al*. 2007), and mouse tissue (Li *et al*. 1999).

The down-regulation of a PIWI-like protein in bleached *M. faveolata* (experiment 1) further supports the notion of increased TE activity during thermal stress. Recent research

in *Drosophila* has shown that PIWI and related proteins are involved in the silencing of retrotransposons. Vagin *et al*. (2006) showed that transposon silencing in the *Drosophila* germ line functioned through repeat-associated small-interfering RNAs that require members of the PIWI subfamily to operate. Mutation of PIWI resulted in the activation of an endogenous retrotransposon in the testes of *Drosophila* (Kalmykova *et al*. 2005). These findings suggest that transposon activation during thermal stress in *M. faveolata* may be due to the down-regulation of PIWI-like proteins.

The above hypothesis of heat-induced TE activity assumes that the microarray probe sequences represent mobile genetic elements present in the coral genome; however, it is not clear where the viral genes come from. An alternative hypothesis for the seemingly increased activity of TEs is that a proliferation of viruses within the coral host and/or symbiotic algae occurs during thermal stress. Viral proliferation in response to thermal stress (Wilson *et al*. 2001) and UV exposure (Lohr *et al*. 2007) has been documented in *Symbiodinium*, and viral-like particles were found to be more abundant in heat-stressed corals compared to controls (Wilson *et al*. 2005). Additionally, the presence of viruses within corals has been found using microscopic (Patten *et al*. 2008) and bioinformatics techniques (Marhaver *et al*. 2008). If the microarray results represent heat-induced viral proliferation, then viral sequences must have been cloned during cDNA library construction. Given that an oligo-dT primer was used to target coral mRNAs, it is unlikely (though not impossible) that viral genomes were cloned.

Conclusions

Overall, the findings presented here represent the first medium-scale transcriptomic study focused on elucidating the molecular and cellular foundation of thermal stress-induced coral bleaching. The results suggest that, as a consequence of thermal stress, corals undergo: a heat shock response, oxidative stress, modifications to the cytoskeleton, decreased calcification, decreased metabolism, increased transposon activity, and transcription and translation modifications. The hypothesis that oxidative stress leads to a disruption of intracellular Ca^{2+} homeostasis is powerful, as it would explain why coral bleaching results in cytoskeletal modifications, changes in cell adhesion properties, and the initiation of cell death via apoptosis and necrosis (Fig. 3). We hope that the differentially expressed genes reported here will be evaluated as to their potential to serve as field-based biomarkers for coral health, and as a starting point for protein-level expression, localization, and functional studies (e.g. the SCRiPs, PXDN, Galaxin, FKBP12, PIWI, EF-hand, and C/EBPβ). Future microarray studies on bleaching induced by light, darkness, and/or synergistic factors (e.g. heat and light) will provide further insights into the molecular mechanisms underlying bleaching. Time course studies, while more complex, are important in order to study the temporal patterns of gene expression that produce the bleaching response. Early time points (minutes to hours) are also necessary as large cellular changes are likely to occur on this timescale.

Acknowledgements

We would like to thank the following people associated with STRI in Panamá: Rachel Collin, Gabriel Jácome, Plínio Gondola and other staff at the Bocas del Toro station, and Eyda Gomez and Javier Jara of Nancy Knowlton's laboratory at the Naos Laboratory. We would also like to thank Adam Carroll at UCSF for training and aid in printing microarrays. The comments of three anonymous reviewers are also greatly appreciated. This paper was prepared by Michael DeSalvo in partial fulfillment of requirements for a Ph.D. in Quantitative and Systems Biology from the University of California, Merced. This study was supported through a STRI Pre-doctoral Fellowship to Michael DeSalvo and NSF awards to Mónica Medina (BE-GEN 0313708 and IOS 0644438). This is contribution #1 of the STRI Caribbean Reef Futures initiative.

References

Abele D, Heise K, Portner HO, Puntarulo S (2002) Temperature-dependence of mitochondrial function and production of reactive oxygen species in the intertidal mud clam *Mya arenaria*. *Journal of Experimental Biology*, **205**, 1831–1841.

Agrawal N, Kango M, Mishra A, Sinha P (1995) Neoplastic transformation and aberrant cell–cell interactions in genetic mosaics of lethal (2) giant larvae (lgl), a tumor suppressor gene of *Drosophila*. *Developmental Biology*, **172**, 218–229.

Allemand D, Tambutte E, Girard JP, Jaubert J (1998) Organic matrix synthesis in the scleractinian coral *Stylophora pistillata*: role in biomineralization and potential target of the organotin tributyltin. *Journal of Experimental Biology*, **201** (Pt 13), 2001–2009.

Allemand D, Ferrier-Pages C, Furla P *et al*. (2004) Biomineralisation in reef-building corals: from molecular mechanisms to environmental control. *Comptes Rendus Palevol*, **3**, 453–467.

Bell J, Neilson L, Pellegrini M (1988) Effect of heat shock on ribosome synthesis in *Drosophila melanogaster*. *Molecular and Cellular Biology*, **8**, 91–95.

Berkelmans R, Oliver JK (1999) Large-scale bleaching of corals on the Great Barrier Reef. *Coral Reefs*, **18**, 55–60.

Black N, Voellmy R, Szmant A (1995) Heat shock protein induction in *Montastraea faveolata* and *Aiptasia pallida* exposed to elevated temperatures. *Biological Bulletin*, **188**, 234–240.

Bou-Abdallah F, Chasteen ND, Lesser MP (2006) Quenching of superoxide radicals by green fluorescent protein. *Biochimica et Biophysica Acta*, **1760**, 1690–1695.

Brown BE, Letissier MDA, Bythell JC (1995) Mechanisms of bleaching deduced from histological studies of reef corals sampled during a natural bleaching event. *Marine Biology*, **122**, 655–663.

Brown BE, Dunne RP, Goodson MS, Douglas AE (2002) Experience shapes the susceptibility of a reef coral to bleaching. *Coral Reefs*, **21**, 119–126.

Brummelkamp TR, Nijman SM, Dirac AM, Bernards R (2003) Loss of the cylindromatosis tumour suppressor inhibits apoptosis by activating NF-kappaB. *Nature*, **424**, 797–801.

Brummendorf T, Kenwrick S, Rathjen FG (1998) Neural cell recognition molecule L1: from cell biology to human hereditary brain malformations. *Current Opinion in Neurobiology*, **8**, 87–97.

Buckley BA, Gracey AY, Somero GN (2006) The cellular response to heat stress in the goby *Gillichthys mirabilis*: a cDNA microarray and protein-level analysis. *Journal of Experimental Biology*, **209**, 2660–2677.

Cadenas E, Davies KJ (2000) Mitochondrial free radical generation, oxidative stress, and aging. *Free Radical Biology and Medicine*, **29**, 222–230.

Chandra D, Choy G, Daniel PT, Tang DG (2005) Bax-dependent regulation of Bak by voltage-dependent anion channel 2. *Journal of Biological Chemistry*, **280**, 19051–19061.

Cheng EH, Sheiko TV, Fisher JK, Craigen WJ, Korsmeyer SJ (2003) VDAC2 inhibits BAK activation and mitochondrial apoptosis. *Science*, **301**, 513–517.

Coles SL, Jokiel PL (1978) Synergistic effects of temperature, salinity and light on the hermatypic coral Montipora verrucosa. *Marine Biology*, **V49**, 187–195.

Covarrubias MY, Khan RL, Vadigepalli R, Hoek JB, Schwaber JS (2005) Chronic alcohol exposure alters transcription broadly in a key integrative brain nucleus for homeostasis: the nucleus tractus solitarus. *Physiological Genomics*, **24**, 45–58.

Cui X, Hwang JT, Qiu J, Blades NJ, Churchill GA (2005) Improved statistical tests for differential gene expression by shrinking variance components estimates. *Biostatistics*, **6**, 59–75.

Cuif JP, Dauphin Y, Freiwald A, Gautret P, Zibrowius H (1999) Biochemical markers of zoaxanthellae symbiosis in soluble matrices of skeleton of 24 *Scleractinia* species. *Comparative Biochemistry and Physiology A: Molecular and Integrative Physiology*, **123**, 269–278.

Dallas PB, Gottardo NG, Firth MJ *et al*. (2005) Gene expression levels assessed by oligonucleotide microarray analysis and quantitative real-time RT-PCR – how well do they correlate? *BMC Genomics*, **6**, 59.

Davidson JF, Schiestl RH (2001) Mitochondrial respiratory electron carriers are involved in oxidative stress during heat stress in *Saccaromyces cerevisiae*. *Molecular and Cellular Biology*, **21**, 8483–8489.

Davidson JF, Whyte B, Bissinger PH, Schiestl RH (1996) Oxidative stress is involved in heat-induced cell death in *Saccaromyces cerevisiae*. *Proceedings of the National Academy of Sciences, USA*, **93**, 5116–5121.

de la Vega E, Degnan BM, Hall MR, Wilson KJ (2007) Differential expression of immune-related genes and transposable elements in black tiger shrimp (*Panaeus monodon*) exposed to a range of environmental stressors. *Fish & Shellfish Immunology*, **23**, 1072–1088.

Delon I, Brown NH (2007) Integrins and the actin cytoskeleton. *Current Opinion in Cell Biology*, **19**, 43–50.

Douglas AE (2003) Coral bleaching – how and why? *Marine Pollution Bulletin*, **46**, 385–392.

Dove S, Carlos Ortiz J, Enriquez S *et al*. (2006) Response of the holosymbiont pigments from the scleractinian coral *Montipora monasteriata* to short-term heat stress. *Limnology and Oceanography*, **51**, 1149–1158.

Downs CA, Mueller E, Phillips S, Fauth JE, Woodley CM (2000) A molecular biomarker system for assessing the health of coral (*Montastraea faveolata*) during heat stress. *Marine Biotechnology*, **2**, 533–544.

Downs CA, Fauth JE, Halas JC *et al*. (2002) Oxidative stress and seasonal coral bleaching. *Free Radical Biology and Medicine*, **33**, 533–543.

Downs CA, Fauth JE, Robinson CE *et al*. (2005) Cellular diagnostics and coral health: declining coral health in the Florida Keys. *Marine Pollution Bulletin*, **51**, 558–569.

Duchen MR (2000) Mitochondria and calcium: from cell signalling to cell death. *Journal of Physiology*, **529** (Pt 1), 57–68.

Dunn SR, Bythell JC, Le Tissier MDA, Burnett WJ, Thomason JC (2002) Programmed cell death and cell necrosis activity during hyperthermic stress-induced bleaching of the symbiotic sea anemone *Aiptasia* sp. *Journal of Experimental Marine Biology and Ecology*, **272**, 29–53.

Dunn SR, Thomason JC, Le Tissier MD, Bythell JC (2004) Heat stress induces different forms of cell death in sea anemones and their endosymbiotic algae depending on temperature and duration. *Cell Death and Differentiation*, **11**, 1213–1222.

Dunn SR, Phillips WS, Spatafora JW, Green DR, Weis VM (2006) Highly conserved caspase and Bcl-2 homologues from the sea anemone *Aiptasia pallida*: lower metazoans as models for the study of apoptosis evolution. *Journal of Molecular Evolution*, **63**, 95–107.

Dunn SR, Schnitzler CE, Weis VM (2007) Apoptosis and autophagy as mechanisms of dinoflagellate symbiont release during cnidarian bleaching: every which way you lose. *Proceedings of the Royal Society B: Biological Sciences*, **274**, 3079–3085.

Edge SE, Morgan MB, Gleason DF, Snell TW (2005) Development of a coral cDNA array to examine gene expression profiles in *Montastraea faveolata* exposed to environmental stress. *Marine Pollution Bulletin*, **51**, 507–523.

Etienne W, Meyer MH, Peppers J, Meyer RA (2004) Comparison of mRNA gene expression by RT-PCR and DNA microarray. *BioTechniques*, **36**, 618–626.

Fang LS, Huang SP, Lin KL (1997) High temperature induces the synthesis of heat-shock proteins and the elevation of intracellular calcium in the coral *Acropora grandis*. *Coral Reefs*, **16**, 127–131.

Fill M, Copello JA (2002) Ryanodine receptor calcium release channels. *Physiological Reviews*, **82**, 893–922.

Fitt WK, Warner ME (1995) Bleaching patterns of four species of Caribbean reef corals. *Biological Bulletin*, **189**, 298–307.

Fukuda I, Ooki S, Fujita T *et al*. (2003) Molecular cloning of a cDNA encoding a soluble protein in the coral exoskeleton. *Biochemical and Biophysical Research Communications*, **304**, 11–17.

Gateff E (1978) Malignant neoplasms of genetic origin in *Drosophila melanogaster*. *Science*, **200**, 1448–1459.

Gates RD, Edmunds PJ (1999) The physiological mechanisms of acclimatization in tropical reef corals. *American Zoologist*, **39**, 30–43.

Gates RD, Baghdasarian G, Muscatine L (1992) Temperature stress causes host cell detachment in symbiotic cnidarians: implications for coral bleaching. *Biological Bulletin*, **182**, 324–332.

Gibson G (2002) Microarrays in ecology and evolution: a preview. *Molecular Ecology*, **11**, 17–24.

Gleason DF, Wellington GM (1993) Ultraviolet-radiation and coral bleaching. *Nature*, **365**, 836–838.

Glynn PW (1993) Coral-reef bleaching – ecological perspectives. *Coral Reefs*, **12**, 1–17.

Glynn PW, Peters EC, Muscatine L (1985) Coral tissue microstructure and necrosis – relation to catastrophic coral mortality in Panama. *Diseases of Aquatic Organisms*, **1**, 29–37.

Glynn PW, Mate JL, Baker AC, Calderon MO (2001) Coral bleaching and mortality in Panama and Ecuador during the 1997–98 El Nino-Southern Oscillation event: spatial/temporal patterns and comparisons with the 1982–83 event. *Bulletin of Marine Science*, **69**, 79–109.

Goreau T, McClanahan T, Hayes R, Strong A (2000) Conservation

of coral reefs after the 1998 global bleaching event. *Conservation Biology*, **14**, 5–15.

Gracey AY, Cossins AR (2003) Application of microarray technology in environmental and comparative physiology. *Annual Review of Physiology*, **65**, 231–259.

Gracey AY, Troll JV, Somero GN (2001) Hypoxia-induced gene expression profiling in the euryoxic fish *Gillichthys mirabilis*. *Proceedings of the National Academy of Sciences, USA*, **98**, 1993–1998.

Hajnoczky G, Davies E, Madesh M (2003) Calcium signaling and apoptosis. *Biochemical and Biophysical Research Communications*, **304**, 445–454.

Halbleib JM, Nelson WJ (2006) Cadherins in development: cell adhesion, sorting, and tissue morphogenesis. *Genes and Development*, **20**, 3199–3214.

Harvell CD, Kim K, Burkholder JM *et al*. (1999) Emerging marine diseases – climate links and anthropogenic factors. *Science*, **285**, 1505–1510.

Hawkins RD, Bashiardes S, Powder KE *et al*. (2007) Large scale gene expression profiles of regenerating inner ear sensory epithelia. *PLoS ONE*, **2**, e525.

Hayes RL, King CM (1995) Induction of 70-kD heat shock protein in scleractinian corals by elevated temperature: significance for coral bleaching. *Molecular Marine Biology and Biotechnology*, **4**, 36–42.

Hayes JD, McLellan LI (1999) Glutathione and glutathione-dependent enzymes represent a co-ordinately regulated defence against oxidative stress. *Free Radical Research*, **31**, 273–300.

Herruer MH, Mager WH, Raue HA *et al*. (1988) Mild temperature shock affects transcription of yeast ribosomal protein genes as well as the stability of their mRNAs. *Nucleic Acids Research*, **16**, 7917–7929.

Hidalgo C (2005) Cross talk between Ca2+ and redox signalling cascades in muscle and neurons through the combined activation of ryanodine receptors/Ca2+ release channels. *Philosophical Transactions of the Royal Society of London. Series B: Biological Sciences*, **360**, 2237–2246.

Hoegh-Guldberg O (1999) Climate change, coral bleaching and the future of the world's coral reefs. *Marine and Freshwater Research*, **50**, 839–866.

Hoegh-Guldberg O, Smith GJ (1989) The effect of sudden changes in temperature, light and salinity on the population density and export of zooxanthellae from the reef corals *Stylophora pistillata* Esper and *Seriatopora hystrix* Dana. *Journal of Experimental Marine Biology and Ecology*, **129**, 279–303.

Hoegh-Guldberg O, Mumby PJ, Hooten AJ *et al*. (2007) Coral reefs under rapid climate change and ocean acidification. *Science*, **318**, 1737–1742.

Hofmann GE, Burnaford JL, Fielman KT (2005) Genomics-fueled approaches to current challenges in marine ecology. *Trends in Ecology & Evolution*, **20**, 305–311.

Holmgren A (1985) Thioredoxin. *Annual Review of Biochemistry*, **54**, 237–271.

Huang SP, Lin KL, Fang LS (1998) The involvement of calcium in heat-induced coral bleaching. *Zoological Studies*, **37**, 89–94.

Hudson JH (1981) Growth rates in *Montastraea annularis* – a record of environmental change in Key Largo Coral Reef Marine Sanctuary, Florida. *Bulletin of Marine Science*, **31**, 444–459.

Hughes TP (1994) Catastrophes, phase shifts, and large-scale degradation of a Caribbean coral reef. *Science*, **265**, 1547–1551.

Hughes TP, Baird AH, Bellwood DR *et al*. (2003) Climate change, human impacts, and the resilience of coral reefs. *Science*, **301**, 929–933.

Iglesias-Prieto R, Matta JL, Robins WA, Trench RK (1992) Photosynthetic response to elevated temperature in the symbiotic dinoflagellate *Symbiodinium microadriaticum* in culture. *Proceedings of the National Academy of Sciences, USA*, **89**, 10302–10305.

Jackson JB, Kirby MX, Berger WH *et al*. (2001) Historical overfishing and the recent collapse of coastal ecosystems. *Science*, **293**, 629–637.

Janmey PA, Stossel TP (1987) Modulation of gelsolin function by phosphatidylinositol 4,5-bisphosphate. *Nature*, **325**, 362–364.

Jokiel PL, Coles SL (1977) Effects of temperature on mortality and growth of Hawaiian reef corals. *Marine Biology*, **43**, 201–208.

Jones R (2005) The ecotoxicological effects of Photosystem II herbicides on corals. *Marine Pollution Bulletin*, **51**, 495–506.

Jones RJ, Hoegh-Guldberg O, Larkum AWD, Schreiber U (1998) Temperature-induced bleaching of corals begins with impairment of the CO2 fixation mechanism in zooxanthellae. *Plant Cell and Environment*, **21**, 1219–1230.

Kalmykova AI, Klenov MS, Gvozdev VA (2005) Argonaute protein PIWI controls mobilization of retrotransposons in the *Drosophila* male germline. *Nucleic Acids Research*, **33**, 2052–2059.

Kasri NN, Parys JB, Callewaert G, Missiaen L, De Smedt H (2004) Calmodulin and calcium-release channels. *Biological Research*, **37**, 577–582.

Kassahn KS, Caley MJ, Ward AC *et al*. (2007) Heterologous microarray experiments used to identify the early gene response to heat stress in a coral reef fish. *Molecular Ecology*, **16**, 1749–1763.

Yu L, Kelly U, Ebright JN *et al*. (2007) Oxidative stress-induced expression and modulation of Phosphatase of Regenerating Liver-1 (PRL-1) in mammalian retina. *Biochimica et Biophysica Acta*, **1773**, 1473–1482.

Kerr MK (2003) Design considerations for efficient and effective microarray studies. *Biometrics*, **59**, 822–828.

Kimura RH, Choudary PV, Stone KK, Schmid CW (2001) Stress induction of Bm1 RNA in silkworm larvae: SINEs, an unusual class of stress genes. *Cell Stress Chaperones*, **6**, 263–272.

Kovalenko A, Chable-Bessia C, Cantarella G *et al*. (2003) The tumour suppressor CYLD negatively regulates NF-kappaB signalling by deubiquitination. *Nature*, **424**, 801–805.

Kushmaro A, Loya Y, Fine M, Rosenberg E (1996) Bacterial infection and coral bleaching. *Nature*, **380**, 396.

Lasker HR, Peters EC, Coffroth MA (1984) Bleaching of reef coelenterates in the San-Blas Islands, Panama. *Coral Reefs*, **3**, 183–190.

Lees-Miller JP, Helfman DM (1991) The molecular basis for tropomyosin isoform diversity. *Bioessays*, **13**, 429–437.

Lesser MP (1996) Elevated temperatures and ultraviolet radiation cause oxidative stress and inhibit photosynthesis in symbiotic dinoflagellates. *Limnology and Oceanography*, **41**, 271–283.

Lesser MP (2006) Oxidative stress in marine environments: biochemistry and physiological ecology. *Annual Review of Physiology*, **68**, 253–278.

Lesser MP, Farrell JH (2004) Exposure to solar radiation increases damage to both host tissues and algal symbionts of corals during thermal stress. *Coral Reefs*, **23**, 367–377.

Lesser MP, Stochaj WR, Tapley DW, Shick JM (1990) Bleaching in coral-reef anthozoans – effects of irradiance, ultraviolet-radiation, and temperature on the activities of protective enzymes against active oxygen. *Coral Reefs*, **8**, 225–232.

Li T, Spearow J, Rubin CM, Schmid CW (1999) Physiological stresses increase mouse short interspersed element (SINE) RNA expression in vivo. *Gene*, **239**, 367–372.

Lindquist S (1986) The heat-shock response. *Annual Review of Biochemistry*, **55**, 1151–1191.

Litjens SH, de Pereda JM, Sonnenberg A (2006) Current insights into the formation and breakdown of hemidesmosomes. *Trends in Cell Biology*, **16**, 376–383.

Livak KJ, Schmittgen TD (2001) Analysis of relative gene expression data using real-time quantitative PCR and the 2 (-Delta Delta C (T) Method. *Methods*, **25**, 402–408.

Lohr J, Munn CB, Wilson WH (2007) Characterization of a latent virus-like infection of symbiotic zooxanthellae. *Applied and Environmental Microbiology*, **73**, 2976–2981.

Loven DP (1988) A role for reduced oxygen species in heat induced cell killing and the induction of thermotolerance. *Medical Hypotheses*, **26**, 39–50.

Marhaver KL, Edwards RA, Rohwer F (2008) Viral communities associated with healthy and bleaching corals. *Environmental Microbiology*, on-line first.

Mayfield AB, Gates RD (2007) Osmoregulation in anthozoan-dinoflagellate symbiosis. *Comparative Biochemistry and Physiology A: Molecular and Integrative Physiology*, **147**, 1–10.

McClintock B (1950) The origin and behavior of mutable loci in maize. *Proceedings of the National Academy of Sciences, USA*, **36**, 344–355.

McClintock B (1984) The significance of responses of the genome to challenge. *Science*, **226**, 792–801.

Morgan MB, Edge SE, Snell TW (2005) Profiling differential gene expression of corals along a transect of waters adjacent to the Bermuda municipal dump. *Marine Pollution Bulletin*, **51**, 524–533.

Muller J, Menzel D, Samaj J (2007) Cell-type specific disruption and recovery of the cytoskeleton in *Arabidopsis thaliana* epidermal root cells upon heat shock stress. *Protoplasma*, **230**, 231–242.

Muscatine L (1990) The role of symbiotic algae in carbon and energy flux in reef corals. In: *Coral Reefs* (ed. Dubinsky Z), pp. 75–87. Elsevier, Amsterdam.

Nicotera P, Leist M, Ferrando-May E (1998) Intracellular ATP, a switch in the decision between apoptosis and necrosis. *Toxicology Letters*, **102–103**, 139–142.

Nijman SM, Luna-Vargas MP, Velds A *et al*. (2005) A genomic and functional inventory of deubiquitinating enzymes. *Cell*, **123**, 773–786.

Orrenius S, Burkitt MJ, Kass GE, Dypbukt JM, Nicotera P (1992) Calcium ions and oxidative cell injury. *Annals of Neurology*, **32** (Suppl.), S33–S42.

Orrenius S, Zhivotovsky B, Nicotera P (2003) Regulation of cell death: the calcium-apoptosis link. *Nature Reviews Molecular Cell Biology*, **4**, 552–565.

Pandolfi JM, Bradbury RH, Sala E *et al*. (2003) Global trajectories of the long-term decline of coral reef ecosystems. *Science*, **301**, 955–958.

Patten NL, Harrison PL, Mitchell JG (2008) Prevalence of virus-like particles within a staghorn scleractinian coral (*Acropora muricata*) from the Great Barrier Reef. *Coral Reefs*, on-line first.

Perez S, Weis V (2006) Nitric oxide and cnidarian bleaching: an eviction notice mediates breakdown of a symbiosis. *Journal of Experimental Biology*, **209**, 2804–2810.

Place SP, O'Donnell MJ, Hofmann GE (2008) Gene expression in the intertidal mussel *Mytilus californianus*: physiological response to environmental factors on a biogeographic scale. *Marine Ecology Progress Series*, **356**, 1–14.

Putnam NH, Srivastava M, Hellsten U *et al*. (2007) Sea anemone genome reveals ancestral eumetazoan gene repertoire and genomic organization. *Science*, **317**, 86–94.

Rajeevan MS, Vernon SD, Taysavang N, Unger ER (2001) Validation of array-based gene expression profiles by real-time (kinetic) RT-PCR. *Journal of Molecular Diagnostics*, **3**, 26–31.

Ratner VA, Zabanov SA, Kolesnikova OV, Vasilyeva LA (1992) Induction of the mobile genetic element Dm-412 transpositions in the *Drosophila* genome by heat shock treatment. *Proceedings of the National Academy of Sciences, USA*, **89**, 5650–5654.

Richier S, Sabourault C, Courtiade J *et al*. (2006) Oxidative stress and apoptotic events during thermal stress in the symbiotic sea anemone, *Anemonia viridis*. *FEBS Journ*, **273**, 4186–4198.

Richter C (1998) Nitric oxide and its congeners in mitochondria: implications for apoptosis. *Environmental Health Perspectives*, **106** (Suppl. 5), 1125–1130.

Riobo NA, Clementi E, Melani M *et al*. (2001) Nitric oxide inhibits mitochondrial NADH: ubiquinone reductase activity through peroxynitrite formation. *Biochemical Journal*, **359**, 139–145.

Rodriguez-Lanetty M, Phillips WS, Weis VM (2006) Transcriptome analysis of a cnidarian-dinoflagellate mutualism reveals complex modulation of host gene expression. *BMC Genomics*, **7**, 23.

Rodriguez-Lanetty M, Phillips WS, Dove S, Hoegh-Guldberg O, Weis VM (2007) Analytical approach for selecting normalizing genes from a cDNA microarray platform to be used in q-RT-PCR assays: a cnidarian case study. *Journal of Biochemical and Biophysical Methods*, **6**, 985–991.

Rowan R, Powers DA (1991) Molecular genetic identification of symbiotic dinoflagellates (zooxanthellae). *Marine Ecology Progress Series*, **71**, 65–73.

Rowan R, Knowlton N, Baker AC, Jara J (1997) Landscape ecology of algal symbiont communities explains variation in episodes of coral bleaching. *Nature*, **388**, 265–269.

Saeed AI, Sharov V, White J *et al*. (2003) TM4: a free, open-source system for microarray data management and analysis. *BioTechniques*, **34**, 374–378.

Salih A, Larkum A, Cox G, Kuhl M, Hoegh-Guldberg O (2000) Fluorescent pigments in corals are photoprotective. *Nature*, **408**, 850–853.

Sawyer SJ, Muscatine L (2001) Cellular mechanisms underlying temperature-induced bleaching in the tropical sea anemone *Aiptasia pulchella*. *Journal of Experimental Biology*, **204**, 3443–3456.

Schallreuter KU, Gibbons NC, Zothner C, Abou Elloof MM, Wood JM (2007) Hydrogen peroxide-mediated oxidative stress disrupts calcium binding on calmodulin: more evidence for oxidative stress in vitiligo. *Biochemical and Biophysical Research Communications*, **360**, 70–75.

Schwarz JA, Brokstein PB, Voolstra C *et al*. (2008) Coral life history and symbiosis: functional genomic resources for two reef building Caribbean corals, *Acropora palmata* and *Montastraea faveolata*. *BMC Genomics*, **9**, 97.

Shapiro SD (1998) Matrix metalloproteinase degradation of extracellular matrix: biological consequences. *Current Opinion in Cell Biology*, **10**, 602–608.

Sharp VA, Brown BE, Miller D (1997) Heat shock protein (hsp 70) expression in the tropical reef coral *Goniopora djiboutiensis*. *Journal of Thermal Biology*, **22**, 11–19.

Shin MH, Moon YJ, Seo J-E *et al*. (2008) Reactive oxygen species produced by NADPH oxidase, xanthine oxidase, and mitochondrial electron transport system mediate heat shock-induced MMP-1 and MMP-9 expression. *Free Radical Biology and Medicine*, **44**, 635–645.

Simonson SJ, Wu ZH, Miyamoto S (2007) CYLD: a DUB with many talents. *Developmental Cell*, **13**, 601–603.

Singh SP, Coronella JA, Benes H, Cochrane BJ, Zimniak P (2001) Catalytic function of *Drosophila melanogaster* glutathione S-transferase DmGSTS1–1 (GST-2) in conjugation of lipid peroxidation end products. *European Journal of Biochemistry*, **268**, 2912–2923.

Smith DJ, Suggett DJ, Baker NR (2005) Is photoinhibition of zooxanthellae photosynthesis the primary cause of thermal bleaching in corals? *Global Change Biology*, **11**, 1–11.

Smith-Keune C, Dove S (2008) Gene expression of a green fluorescent protein homolog as a host-specific biomarker of heat stress within a reef-building coral. *Marine Biotechnology (NY)*, **10**, 166–180.

Sonawane M, Carpio Y, Geisler R *et al*. (2005) Zebrafish penner/lethal giant larvae 2 functions in hemidesmosome formation, maintenance of cellular morphology and growth regulation in the developing basal epidermis. *Development*, **132**, 3255–3265.

Steen RG, Muscatine L (1987) Low-temperature evokes rapid exocytosis of symbiotic algae by a sea-anemone. *Biological Bulletin*, **172**, 246–263.

Strand D, Raska I, Mechler BM (1994) The *Drosophila* lethal (2) giant larvae tumor suppressor protein is a component of the cytoskeleton. *Journal of Cell Biology*, **127**, 1345–1360.

Strychar KB, Coates M, Sammarco PW, Piva TJ (2004) Bleaching as a pathogenic response in scleractinian corals, evidenced by high concentrations of apoptotic and necrotic zooxanthellae. *Journal of Experimental Marine Biology and Ecology*, **304**, 99–121.

Szmant AM, Gassman NJ (1990) The effects of prolonged bleaching on the tissue biomass and reproduction of the reef coral *Montastrea annularis*. *Coral Reefs*, **8**, 217–224.

Tambutte E, Allemand D, Mueller E, Jaubert J (1996) A compartmental approach to the mechanism of calcification in hermatypic corals. *Journal of Experimental Biology*, **199**, 1029–1041.

Teranishi KS, Stillman JH (2007) A cDNA microarray analysis of the response to heat stress in hepatopancreas tissue of the porcelain crab *Petrolisthes cinctipes*. *Comparative Biochemistry and Physiology D-Genomics and Proteomics*, **2**, 53–62.

Tiwari BS, Belenghi B, Levine A (2002) Oxidative stress increased respiration and generation of reactive oxygen species, resulting in ATP depletion, opening of mitochondrial permeability transition, and programmed cell death. *Plant Physiology*, **128**, 1271–1281.

Trapido-Rosenthal H, Zielke S, Owen R *et al*. (2005) Increased zooxanthellae nitric oxide synthase activity is associated with coral bleaching. *Biological Bulletin*, **208**, 3–6.

Trench RK (1979) The cell biology of plant-animal symbiosis. *Annual Review of Plant Physiology*, **30**, 485–531.

Vagin VV, Sigova A, Li C *et al*. (2006) A distinct small RNA pathway silences selfish genetic elements in the germline. *Science*, **313**, 320–324.

van Oppen MJ, Gates RD (2006) Conservation genetics and the resilience of reef-building corals. *Molecular Ecology*, **15**, 3863–3883.

Wang T, Barbacioru C, Hyland F *et al*. (2006) Large scale real-time PCR validation on gene expression measurements from two commercial long-oligonucleotide microarrays. *BMC Genomics*, **7**, 59.

Warner ME, Fitt WK, Schmidt GW (1996) The effects of elevated temperature on the photosynthetic efficiency of zooxanthellae in hospite from four different species of reef coral: a novel approach. *Plant Cell and Environment*, **19**, 291–299.

Warner ME, Fitt WK, Schmidt GW (1999) Damage to photosystem II in symbiotic dinoflagellates: a determinant of coral bleaching. *Proceedings of the National Academy of Sciences, USA*, **96**, 8007–8012.

Weil E, Smith G, Gil-Agudelo DL (2006) Status and progress in coral reef disease research. *Diseases of Aquatic Organisms*, **69**, 1–7.

Wessler SR (1996) Turned on by stress. Plant retrotransposons. *Current Biology*, **6**, 959–961.

Westfall PH, Young SS (1993) On adjusting *P*-values for multiplicity. *Biometrics*, **49**, 941–945.

Wilson WH, Francis I, Ryan K, Davy SK (2001) Temperature induction of viruses in symbiotic dinoflagellates. *Aquatic Microbial Ecology*, **25**, 99–102.

Wilson WH, Dale AL, Davy JE, Davy SK (2005) An enemy within? Observations of virus-like particles in reef corals. *Coral Reefs*, **24**, 145–148.

Wu H, Churchill GA (2005) *J/MAANOVA User Manual*. The Jackson Laboratory, Bar Harbour, ME. URL: http://research.jax.org/faculty/churchill/software/Jmaanova/Jmoanova.pdf/

Wu H, Kerr MK, Cui X, Churchill GA (2003) MAANOVA: a software package for the analysis of spotted cDNA microarray experiments. In: *The Analysis of Gene Expression Data Methods and Software* (eds Giovanni Parmigiani ESG, Irizarry RA, Zeger SL), pp. 313–341. Springer-Verlag, New York.

Xue L, Igaki T, Kuranaga E *et al*. (2007) Tumor suppressor CYLD regulates JNK-induced cell death in *Drosophila*. *Developmental Cell*, **13**, 446–454.

Yuen T, Wurmbach E, Pfeffer RL, Ebersole BJ, Sealfon SC (2002) Accuracy and calibration of commercial oligonucleotide and custom cDNA microarrays. *Nucleic Acids Research*, **30**, e48.

All of the authors focus on transcriptomic responses of marine organisms to the environment and to other organisms, such as symbionts. Michael DeSalvo is a PhD candidate in the lab of Mónica Medina working closely with labmates Christian Voolstra (post-doc) and Shinichi Sunagawa (PhD candidate). Jodi Schwarz is a past member of the Medina lab. A major goal of the Medina lab is to study the onset, maintenance, and breakdown of the coral-algal symbiosis using microarrays. This research is performed in collaboration with Mary Alice Coffroth (population dynamics and early ontogeny of coral-algal symbioses) and Alina Szmant (coral physiology and reproductive biology). Jonathon Stillman is a marine environmental physiologist who incorporates functional genomics in his projects.

Supplementary material

The following supplementary material is available for this article:

Table S1 qRT–PCR primers used to amplify seven differentially expressed genes and one housekeeping gene (CAON1295)

Table S2 All 309 differentially expressed genes from experiment 1, a replicate ($n = 5$) dye-swap experiment comparing gene expression between partially bleached and control *Montastraea faveolata* fragments

Table S3 All 280 differentially expressed genes from experiment 2, a replicate ($n = 4$) time course experiment (experiment 2) containing four time points. Expression values in columns E-H represent $\log_2$ ratios. Cluster assignments are based on *K*-means clustering with eight defined groups

Table S4 The 57 genes that were consistently differentially expressed in both experiments 1 and 2. Column E is the fold change difference between the time zero and partially bleached time points in experiment 2. This figure should be compared to Column F – the fold change reported in experiment 1

Table S5 The variance in gene expression between the five fragments of each condition (control vs. heat-stressed) and the two technical replicates for each microarray hybridization in experiment 1. Expression data are reported as $\log_2$/lowess transformed intensities for the seven genes validated using qRT–PCR plus six additional differentially expressed genes

This material is available as part of the online article from:
http://www.blackwell-synergy.com/doi/abs/10.1111/j.1365-294X.2008.03879.x
(This link will take you to the article abstract).